

# EMISSIONS REDUCTION ALBERTA



## Project Final Report

**ERA Project ID:** F101150  
**Project Title:** Effective Solvent Extraction Incorporating Electromagnetic Heating (ESEIEH®)

**R45245ecipient Contact:** Paul Morris, Suncor Energy Inc.  
[pamorris@suncor.com](mailto:pamorris@suncor.com)  
(403-296-3154)

**ERA Project Advisor:** Bruce Duong

**Completion Date:** December 31, 2021

**Total ERA Funds Received:** \$16,474,830

**Submission Date:** 19 August, 2022

---

**Table of Contents**

A. Executive Summary ..... 5

B. Overall Project Objectives ..... 7

*Project Phases* ..... 9

C. Phase 1 Mine Face Test ..... 10

*Introduction*..... 10

*Coupled Electromagnetic Reservoir Simulator (CEMRS)* ..... 10

*Test Site and Equipment* ..... 12

*Numerical Model of the Mine Face Test* ..... 15

*Test Results and Discussion* ..... 18

*Numerical Model Results*..... 20

*Post Test Analyses*..... 25

D. Phase 2 Small Scale (In-situ) Demonstration ..... 29

*Introduction*..... 29

*Test Site* ..... 30

*Well Design* ..... 30

*Well Placement* ..... 32

*Coupled Electromagnetic Reservoir Simulator (CEMRS)* ..... 33

*Facilities*..... 34

*Pilot Operations* ..... 35

E. Phase 3 Restart ..... 36

*Phase 2 Investigation*..... 36

*Phase 3 Redesign Activities* ..... 37

*RCA* ..... 42

*Proposed Restart*..... 45

*Mitigation Testing* ..... 45

*Post-Partner Funding Period* ..... 46

F. Overall Conclusions ..... 47

*Scientific Achievements* ..... **Error! Bookmark not defined.**

*Next Steps* ..... 54

*Communications Plan* ..... 55

## List of Figures

FIGURE 1: SAGD VERSUS ESEIEH® YEARLY GHG EMISSIONS. SHADING SHOWS A HIGH-LOW RANGE .....	7
FIGURE 2: ESEIEH® WELL LAYOUT.....	8
FIGURE 3: ESEIEH® PROCESS (US 8,616,273).....	9
FIGURE 4: GRAPHICAL REPRESENTATION OF THE COUPLING BETWEEN THE EM AND RESERVOIR SOLVERS .....	11
FIGURE 5: COMPARISON OF CEMRS TEMPERATURE PROFILES OVER A 10 DAY PERIOD COMPARED TO THE MATHCAD® SOLUTION .....	12
FIGURE 6: MINE FACE TEST SITE LOCATION (DENOTED BY GREEN STAR) .....	12
FIGURE 7: CORE PHOTOS OF THE TEST SITE. THE RED CIRCLE MARKS THE POSITION OF THE ANTENNA .....	13
FIGURE 8: AERIAL VIEW OF THE LAYOUT OF THE ANTENNA AND INSTRUMENTATION BORES FOR THE MINE FACE EXPERIMENT ..	14
FIGURE 9: INSTALLATION OF THE DIPOLE ANTENNA.....	14
FIGURE 10: LAYOUT OF THE SURFACE FACILITIES.....	15
FIGURE 11: RESERVOIR MODEL DOMAIN (A) AXIAL VIEW OF HORIZONTAL PERMEABILITY, (B) TOP VIEW OF INITIAL OIL SATURATION AT THE ANTENNA ELEVATION (DISTANCE UNITS = M).....	16
FIGURE 12: EM MODEL OF THE ANTENNA AND OIL SANDS.....	17
FIGURE 13: CONDUCTIVITY OF THE FORMATION VS. RELATIVE DEPTH FROM ANTENNA CENTERLINE (CL). THE ANTENNA IS POSITIONED AT RELATIVE DEPTH 0 M .....	18
FIGURE 14: POWER SCHEDULE PROVIDED BY THE ANTENNA .....	19
FIGURE 15: SURFACE PLOTS OF THE TEMPERATURE FIELD EVOLUTION AT THE VERTICAL A) OB2 AND B) OB3 WELLS .....	20
FIGURE 16: TEMPERATURE PROFILES FROM VERTICAL OBSERVATION WELLS A) OB2, B) OB3.....	20
FIGURE 17: COMPARISON OF BASELINE CEMRS MODEL WITH TEST DATA FROM DAY 2 TO DAY 20 (A) OB2, (B) OB3 .....	21
FIGURE 18: COMPARISON OF BASELINE CEMRS MODEL WITH TEST DATA FROM DAY 20 TO DAY 43 (A) OB2, (B) OB3 .....	21
FIGURE 19: COMPARISON OF ADJUSTED CEMRS MODEL WITH TEST DATA FROM DAY 2 TO DAY 20 (A) OB2, (B) OB3.....	22
FIGURE 20: COMPARISON OF THE ADJUSTED CEMRS MODEL WITH TEST DATA FROM DAY 20 TO DAY 43 (A) OB2, (B) OB3....	23
FIGURE 21: PREDICTED WATER SATURATION AT DAY 33 FROM AXIAL VIEW AT THE ANTENNA CENTER (RED DOT MARKS THE ANTENNA POSITION, DISTANCE UNITS = M).....	23
FIGURE 22: PROJECTED TEMPERATURE FIELD AFTER 60 DAYS OF 4 kW/M HEATING AT 6.78 MHZ FROM AXIAL VIEW AT THE ANTENNA CENTER.....	24
FIGURE 23: VIEW AT THE BOREHOLE ENTRANCE ACCOMPANIED BY AUDIBLE FLUID SOUNDS EMANATING FROM THE OPENING...25	25
FIGURE 24: SAMPLE FROM THE BOREHOLE ENTRANCE TRANSFERRED TO ANOTHER CONTAINER. SAMPLE TEMPERATURE AT THE POUR TIME WAS 4.5°C (40°F).....	26
FIGURE 25: SAMPLE FROM THE BOREHOLE ENTRANCE TRANSFERRED TO ANOTHER CONTAINER. SAMPLE TEMPERATURE AT THE POUR TIME WAS 4.5°C (40°F).....	26
FIGURE 26: VISCOSITY OF MINE FACE TEST PRODUCED FLUID COMPARED TO ATHABASCA BITUMEN (TYPICAL).....	27
FIGURE 27: SAMPLE COMPOSITIONS FROM THE MINE FACE TEST PRODUCED FLUID COMPARED TO ATHABASCA BITUMEN (TYPICAL) .....	28
FIGURE 28: ESEIEH® TEST SITE.....	30
FIGURE 29: ESEIEH® PHASE II ANTENNA/INJECTOR (EZI-1).....	31
FIGURE 30: HANDLING TEST .....	31
FIGURE 31: WELL PLACEMENTS .....	32
FIGURE 32: EZOB-6 CORE AND WELL PAIR PLACEMENTS .....	32
FIGURE 33: ESEIEH® SMALL SCALE PILOT FACILITIES .....	34
FIGURE 34: START-UP TEMPERATURE PROFILES IN DEGREES CELSIUS (CENTER POINT) .....	35
FIGURE 35: REVISED DESIGN - ESEIEH® PHASE II ANTENNA/INJECTOR (EZI-1).....	37
FIGURE 36: REVISED DESIGN - ESEIEH® PHASE II SOLVENT INJECTION SITE (EZI-2) .....	37
FIGURE 37: REVISED SCHEDULE FROM JAN 2019 MPR.....	39
FIGURE 38: PLANNED RESTART POWER RAMP FROM JAN 2019 MPR.....	40
FIGURE 39: ACTUAL POWER PROFILE FROM 2019 RESTART .....	40
FIGURE 40: LINER TEMPERATURE PROFILE 2019 RESTART .....	41
FIGURE 41: PRODUCER TEMPERATURE PROFILE FROM 2019 RESTART .....	42
FIGURE 42: ISOLATOR DAMAGE FROM 2019 RESTART .....	44
FIGURE 43: ESEIEH(R) GHG FACTOR SENSITIVITIES .....	48
FIGURE 44: TERRAVENT ENVIRONMENTAL NEXT STEPS.....	55

**List of Tables**

TABLE 1: FINAL PARAMETER VALUES USED FOR CEMRS MODEL OF THE MINE FACE TEST .....17  
TABLE 2: 2019 RCA MAJOR ACTIVITIES .....43  
TABLE 3: PROJECT RELATED PATENTS .....53  
TABLE 4: PROJECT RELATED PUBLICATIONS .....54

**List of Attachments**

- [ERA Final Outcomes Report Guidance V2 January 2022](#)
- [SPE-180729-MS: Reducing Supply Cost With ESEIEH™ Pronounced Easy](#)
- [ESEIEH RCA 2018 Technical Committee Rev2\\_0](#)
- [20191014 ESEIEH Low Power RCA Failure Replication Report](#)
- [Evaluation of energy and GHG emissions for ESEIEH](#)

## A. Executive Summary

The goal of the ESEIEH<sup>®</sup> technology is to replace steam for in situ bitumen extraction with electromagnetic heating in combination with solvent dilution. The ESEIEH<sup>®</sup> process eliminates the need for steam, while providing an improved framework for significant reduction in carbon emissions. By some estimates, on a full cycle basis, GHG emissions may be reduced by greater than 80% from steam-assisted gravity drainage with the potential, through the use of renewable energy sources, to approach zero GHG production.

By eliminating steam with its large infrastructure, reducing GHG's and their associated taxes and facilitating the potential for power arbitrage, it is expected that ESEIEH<sup>®</sup>, when proven, will reduce the overall production capital and operating costs, relative to an equivalently sized SAGD development. The potential for increased production rates of a higher product quality is also anticipated to increase revenues and potential clients for the ESEIEH<sup>®</sup> produced product. The combination of these factors would increase global competitiveness and market size thereby offering significant economic advantages to Alberta. Indeed, cost reduction activities undertaken post SPE Paper release in 2016 (SPE-180729-MS, Table 4) including the preliminary design of a "For-Purpose" Transmitter, system architecture simplification, and other opportunities have identified a series of reductions in both capital and operating costs which have reduced the projected costs from 2016 by more than a third.

These positive impacts (reduced GHG emissions, water consumption, land disturbance, etc)) will also be reflected within the society as well. Electrically based production methods will require skilled tradesmen, engineers with advanced degrees in Electrical Engineering and Electromagnetics in addition to the extant requirements for Mechanical, Reservoir, and Process Engineers. New service companies, producers and research areas will emerge (a number have since the project was initiated).

Though the project did not achieve its full potential, a number of significant advancements were made:

- The Mine Face Test (MFT within this document) advanced the technology TRL level from 3 to 5 (on the NASA scale)
- Phase 2 further advanced the system technology to TRL 7 with a single component remaining at TRL4/5 (Center Isolator). The updated component solution was proven in lab-scale testing just prior to the coronavirus shut down. Post coronavirus budget priority changes have resulted in reallocation of funds originally targeted for the field-testing of the component solution.
- Both the Mine Face Test (MFT) and Phase 2 validated electromagnetic energy penetration into native, heterogeneous oil sands. The energy penetration and effects (how hot, how far, how long) occurred in the MFT as modeled. The proven modeling is used for bitumen recovery data, which indicates significant recovery rate, cost and GHG advantages over SAGD. Simulations of more current system architectures indicate even lower energy requirements (0.9 GJ/BBL).
- The project also completed the first field validation of a simulation tool (CEMRS™) capable of predicting temperature profiles, penetration and heating rates by electromagnetic energy in a hydrocarbon resource
- The MFT demonstrated a difference in produced fluid properties than that anticipated
- On the facilities and operational fronts, the project demonstrated the use of standard facility design processes and materials in surface and subsurface systems, documented safety procedures and protocols, and operational constructs for electromagnetic systems
- There was also a significant volume of technical innovation as documented in Table 3, Project Related Patents.

Moving forward, the barriers to entry into today's oil markets (industry-wide capital deployment towards dividends and stock buybacks has increased while R&D spend has decreased) present

significant issues in advancing any EM technology into commerciality. Certainly, today's barriers are far greater than when the ESEIEH<sup>®</sup> pilot was envisioned.

As the global energy crisis continues, these barriers may decrease. Despite the scale and potential of the oil and bitumen markets, TerraVent Environmental Inc. ("**TerraVent**") plans to focus primarily on other markets that may benefit from the application of the project's advancements (among others); for example, mining. In the absence of external funding to complete development and scale marketing efforts, the financial risk of investment under the current market conditions is simply too high. When market conditions become more favorable, or external funding, private or government, are secured, TerraVent will continue development in O&G, ideally with the benefit of additional learnings from other market applications.

From the Operator's Perspective, the physics of the process where energy meets reservoir is complex (high e-field gradients, precise materials & manufacturing, uncertain geology and fluids, and phase change all intersect here). The technical probability of success of the commercial antenna should be risk weighted according to the operator's tolerance.

## B. Overall Project Objectives

### Introduction

The Effective Solvent Extraction Incorporating Electromagnetic Heating ESEIEH<sup>®</sup> process is envisioned as a long-term replacement to the SAGD process. The ESEIEH<sup>®</sup> Process uses a combination of solvent and heat to lower the viscosity of the bitumen, whereas SAGD relies on the steam heating process alone. SAGD emissions intensity is very high – on the order of 70 kg CO<sub>2</sub> / bbl. ESEIEH<sup>®</sup> combines significant GHG reductions (see Figure 1) with cost efficiencies having the potential to dramatically improve on the performance of current practices to produce the provinces vast bitumen resources. The ESEIEH<sup>®</sup> project is a collaboration of that was initiated by four industry petroleum and technology leaders: Laricina Energy Ltd. ("Laricina"), Nexen Inc., Suncor Energy Inc. ("Suncor"), and Harris Corporation, and continued subsequently by Devon Canada Corporation ("Devon"), Nexen Energy ULC (with Nexen Inc. "Nexen"), CNOOC Petroleum North America ULC ("CNOOC"), and Canadian Natural Resources Limited ("CNRL") and L3 Harris Technologies, Inc. (with Harris Corporation ("Harris") (collectively the "Project Participants") with funding support from Alberta Innovates and Emissions Reduction Alberta (ERA).

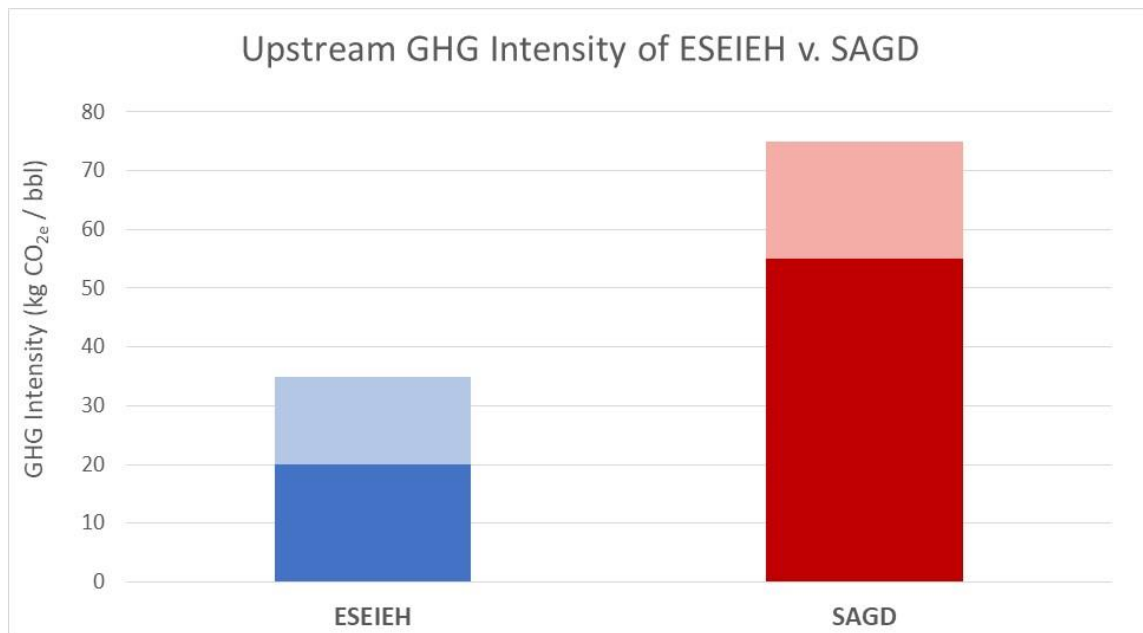


**Figure 1: SAGD versus ESEIEH<sup>®</sup> yearly GHG emissions. Shading shows a high-low range**

The scientific approach forming the basis of the ESEIEH<sup>®</sup> process utilizes electromagnetic (EM) energy to preheat a bitumen reservoir. Application of this alternate energy source eliminates the need for water, water treatment and combustion of natural gas or other hydrocarbon sources for steam generation, bypassing process thermal losses and related GHG emissions.

The Heating ESEIEH<sup>®</sup> recovery process [reference patent] is controlled heating of a bitumen reservoir to a temperature range of 40-70C (example) combined with solvent extraction (see Figure 2 and 3). This provides an improvement over SAGD extraction rates (in simulation) with significantly lower overall energy requirements. The dramatic reduction of process emissions and lower energy requirements combine to create a lower GHG recovery process.

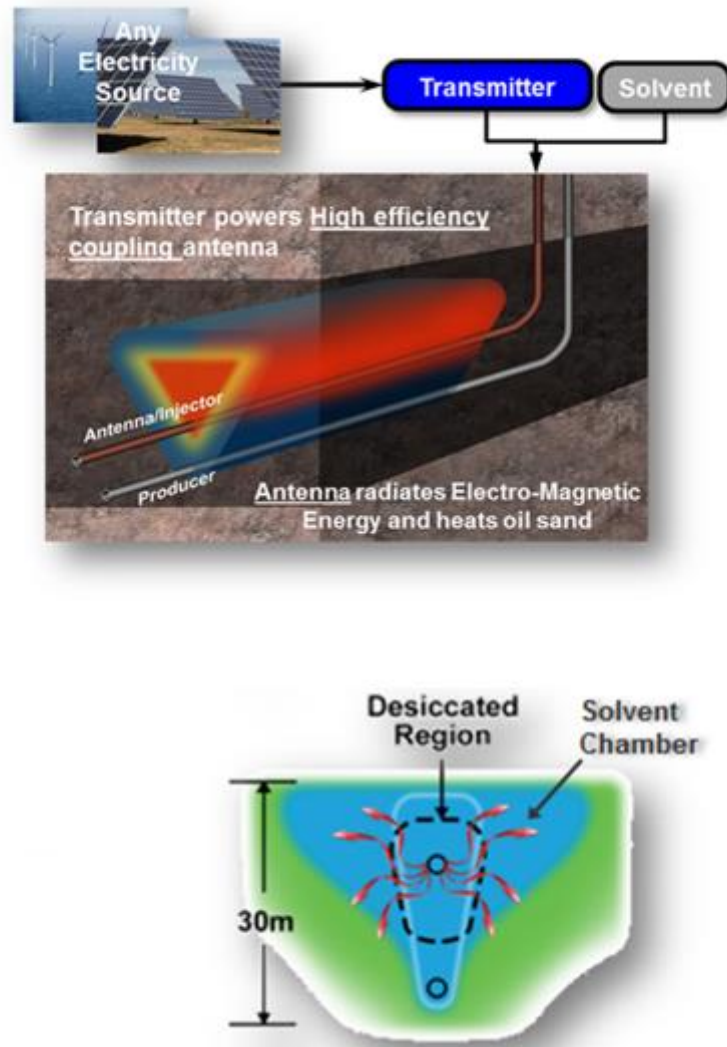
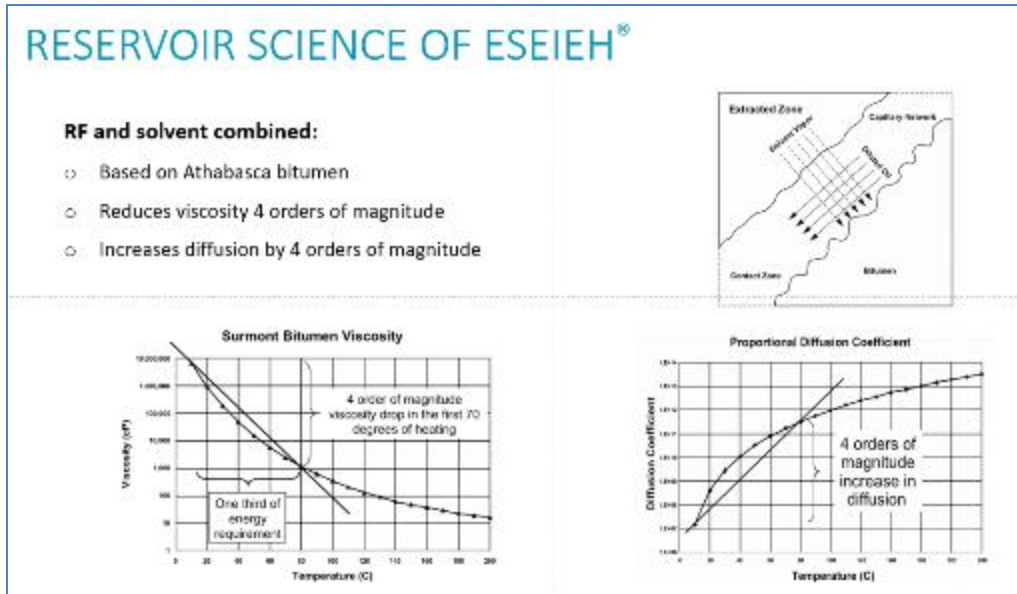


Figure 2: ESEIEH® Well Layout



**Figure 3: ESEIEH<sup>®</sup> Process (US 8,616,273)**

The ERA issues addressed by this project include:

- Pronounced reduction in GHG emissions
- No potable water consumption
- Development of an environmentally benign process for bitumen extraction using alternative energy sources
- Potential reduced diluent requirements for transportation
- Elimination of boiler or coke waste
- Displacement of fossil fuels to centralized facilities where carbon capture and storage can be effectively applied
- Reduced facility/capital/footprints

A successful ESEIEH<sup>®</sup> is an emissions-efficient bitumen extraction technology validated for all in-situ recovery applications. The increased efficiency of ESEIEH<sup>®</sup> can be extended to reservoirs that are non-commercial to SAGD (thin pay, low pressure, middle zones, minimal cap rock, etc.). It may minimize capital and facility investment requirements by extending the life of existing facilities. An economic analysis of the ESEIEH<sup>®</sup> process was presented in [SPE-180729-MS](#) (Reducing Supply Cost With ESEIEH<sup>™</sup> Pronounced Easy). This paper was published in 2016 and indicated a supply cost for ESEIEH<sup>®</sup> of \$50 WTI. Subsequent work conducted within the consortium was conducted to confirm, and in some cases exceed, the assumptions within this analysis. Current models display supply costs below \$50 WTI.

### **Project Phases**

The ESEIEH<sup>®</sup> Project is intended to evaluate the combination of electromagnetic heating for rapid horizontal well pair startup, and sustained formation heating with concurrent injection of a solvent. The

project includes numerical modeling studies, RF hardware design and manufacture, facility design and construction, and two field trials.

The ESEIEH® Project was planned for two phases:

Phase 1 – Proof of Concept of the RF technology: begins with the tasks necessary to define the RF system required for the field pilot test. The end of Phase 1 is the completion of the “Mine Face” test to verify RF energy penetration and absorption rates.

The ESEIEH® Project Team has completed Phase 1 through the successful execution of a mine face test at Suncor’s North Steepbank Mine.

Phase 2 – Small Scale Pilot: includes equipment and facility integration for a technical demonstration with a 100m horizontal well pair and three vertical observation wells that contain the instrumentation necessary to characterize system behavior and analyze the technology’s performance.

### **C. Phase 1 Mine Face Test**

#### ***Introduction***

The mine face test represents the first demonstration of the use of Electromagnetic Heating in an oil recovery process. The project was executed by Nexen, Suncor, Laricina, and Harris with support from Alberta Innovates. The mine face test focused on a proof of concept that RF energy can be effectively used to heat oil sands and that coupled numerical models could adequately predict the results in-situ. The major test objectives were:

- Demonstrate effective equipment installation and system performance.
- Establish antenna performance metrics in oil sands
- Obtain a comprehensive dataset to identify relevant physics of RF heating.
- Provide technology validation for RF reservoir pre-conditioning to a coupled solvent process.

These objectives were demonstrated through the design, deployment, and operation of an RF heating system at a built-for-purpose pit at the North Steepbank Mine. The CEMRS numerical method was validated and the test proved that the hardware could deliver the required lineal power density required for a commercial scale ESEIEH® process.

#### ***Coupled Electromagnetic Reservoir Simulator (CEMRS)***

Harris developed CEMRS in order to address the interdependent relationship between the reservoir composition and the RF heating pattern. It is important to capture this interaction because a change in reservoir composition, for example through desiccation, changes the performance of the RF transducer and the heating from the transducer changes the composition of the reservoir. The reservoir composition also affects the electrical impedance of the antenna. When the transmission line impedance does not match the antenna impedance, a portion of the EM wave reflects from the antenna feed point back onto the transmission line and sets up a Voltage Standing Wave (Ratio), or VSWR. A perfect impedance match has a VSWR of 1 and at large VSWR the increased voltage on the transmission line generates additional heat load along the line and can pose difficulties for operation of the transmitter. The antenna impedance can be managed by selecting an operating frequency that optimizes performance; however, the transmitter has a limited bandwidth and must be designed to function over the anticipated frequency range. The use of coupled EM and reservoir simulators enables the design of a transducer that operates

efficiently over the entire production life of the reservoir. A single operating frequency was used at the mine face test. Up-front CEMRS modeling was used to pre-determine the optimum antenna length. In Phase II the antenna impedance can be managed by adjusting the operating frequency to minimize VSWR.

The coupling process implemented in CEMRS is graphically represented in Figure 4. CEMRS uses Computer Modeling Group, Ltd STARS® thermal reservoir simulator, ANSYS HFSS® EM simulator and a Harris-provided coupling software with built-in electrical material models for oil sands. For this test, an oil sands electrical model [1] was used as a baseline, but was modified to match the resistivity of a well log at the test site.

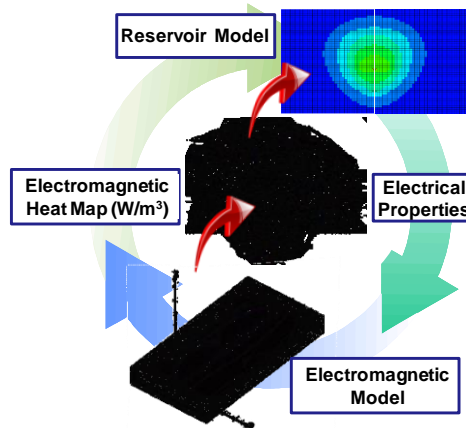


**Figure 4: Graphical representation of the coupling between the EM and reservoir solvers**

The electrical permittivity ( $\epsilon_r$ ) and the conductivity ( $\sigma$ ) of the reservoir must be provided throughout the entire spatial domain of the EM model. The primary variables that affect the electrical properties of the reservoir are the water content, salinity, and temperature. Upon initialization, the reservoir properties are exported to a material model and converted to  $\epsilon_r$  and  $\sigma$  for every tetrahedral element in the EM model. The EM model is provided with a specific antenna design, target operating frequency and appropriate boundary conditions. The EM model is solved and the heat map is interpolated from the finite element mesh onto the reservoir mesh. The reservoir simulator is executed for another time step, updating values for temperature and composition, and then the coupling loop is repeated, explicitly coupling the solvers.

CEMRS was initially validated against a well-defined EM heating problem [2] that could be solved with standard numerical tools. PTC's MATHCAD® was used to solve the differential equations that describe the heat dissipation and thermal response in a 1-D electrically lossy slab as a result of an incident EM plane wave on one surface.

The transient temperature profile was calculated by CEMRS and compared to the MATHCAD® solution for a plane wall geometry of finite thickness with  $\epsilon_r$  of 8 and a  $\sigma$  of 0.01 S/m. In this example, the power density varied spatially but was constant in time. Temperature profiles generated by CEMRS were compared to the MATHCAD® results at several times for thermally insulated boundary conditions.

Figure 5 shows that over a 10 day period the CEMRS predictions were essentially identical to the MATHCAD® results.

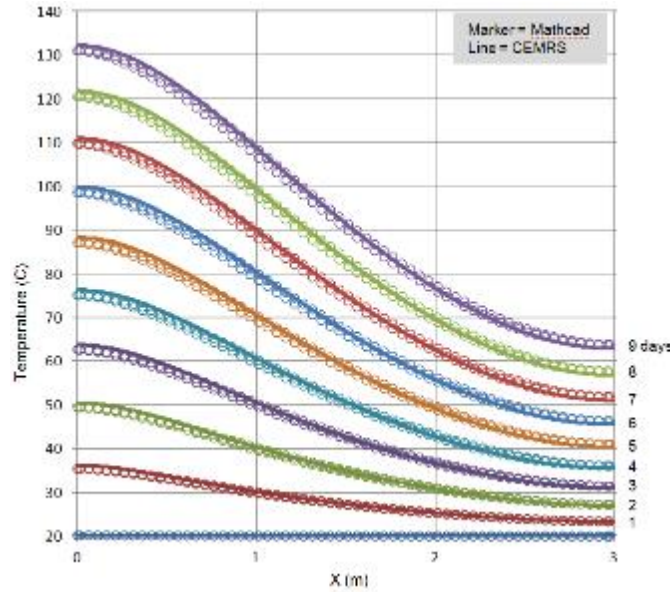


**Figure 5: Comparison of CEMRS temperature profiles over a 10 day period compared to the MATHCAD® solution**

**Test Site and Equipment**

Suncor’s North Steepbank mine was selected as the test site for the first phase of the ESEIEH® project and a built for purpose pit was constructed to provide access to the oil sand layer with a horizontal borehole rig. The specific location and depth of the antenna were determined through an examination of vertical appraisal well logs and core photos from a 2009 drilling program at North Steepbank (see Figure 6). The data showed that the composition of this region was rich oil sand interrupted by inclined hetero-lithic strata (IHS). The antenna was placed at a nominal elevation of 302 m above sea level with approximately 6 m of oil sand and IHS above covered by 5 m of glacial till and 10 m of oil sand and IHS below the antenna. Figure 7 shows the antenna position superimposed on core photos of the interval under test. The photo shows that the region immediately surrounding the antenna was composed of oil sand, mud and shale, which was representative of the heterogeneity of typical Athabasca oil sands.

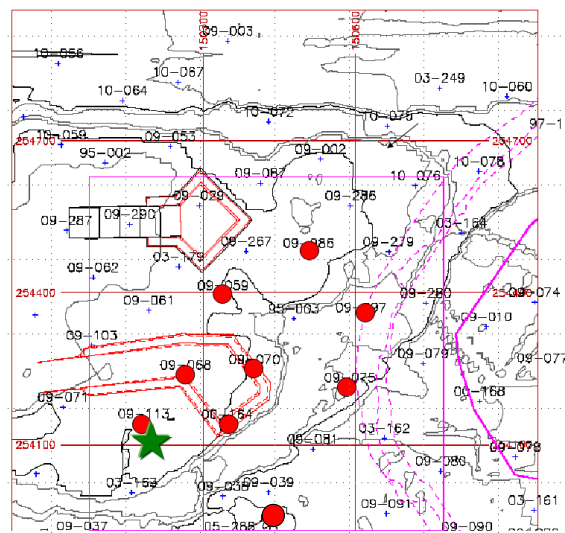


**Figure 6: Mine face test site location (denoted by green star)**

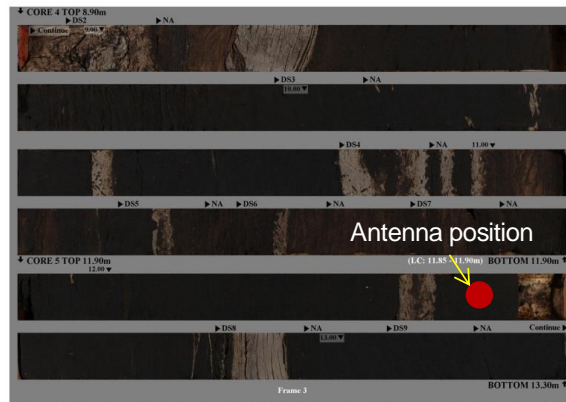


**Figure 7: Core photos of the test site. The red circle marks the position of the antenna**

A physical analysis was conducted on a core that was drilled 0.5 m offset from the center isolator of the antenna which was located approximately 43.5 m from the well flange at the mine face. The formation permeability ranged from 60 mD in a shale layer to as high as 8800 mD in a clean section of oil sand. The porosity ranged from 0.29 to 0.32 and the oil saturation was as high as 0.85 in clean oil sand sections and ranged from 0.26 to 0.5 in IHS layers. Water content measurements of the core samples showed a range of 1.3% to 14.7% and were deemed acceptable for RF heating.

The antenna and instrumentation layout for the experiment is shown in Figure 8. The horizontal bores were drilled to a penetration distance of approximately 59 m from the mine face at a depth of 11 m below the mine surface elevation. The A1 and A2 bores were completed as the primary and backup antenna bores, respectively. Five horizontal and vertical bores were drilled as observation wells. The antenna was installed in A1 inside a 27.3 cm (10.75 in) dielectric casing manufactured by Centron and the center of the antenna was placed 43.5 m from the mine face. The casing was plugged at the toe to prevent intrusion of reservoir materials. A fiberglass casing was chosen to enable the transmission of EM energy into the formation and to allow the antenna to be retrieved if necessary during the test. The cased approach was used in the mine face test primarily for accessibility. Note that the commercial architecture does not require a dielectric casing but utilizes the antenna in direct contact with the reservoir. This risk was mitigated by a series of antenna startups in the Malabar test facility to verify the system could startup and operate in direct contact with oil sands. This program did not anticipate the test startup sequence used in the Phase 2 experiment which was one of the root causes of the subsequent issues. Future efforts are advised to replicate experimental operational conditions in earlier risk mitigation activities instead of projected commercial operational processes as the test processes will, typically, be more stressful to system components. The horizontal and vertical observation wells were built from 11.4 cm (4.5 in) Centron fiberglass tubing to minimize interference with the EM fields that were broadcast from the antenna. All of the wells were instrumented with fiber distributed temperature sensors. The OB1, OB2 and OB3 vertical wells were each fitted with 15 discrete optical temperature sensors (Neoptix OmniFlex™) and these served as the primary sensors for the experiment. The OB1, OB2, and OB3 wells were drilled at an offset of 0.5 m from the edge of the A1 casing. The bores extended below the antenna centerline elevation in order to capture the temperature distribution both above and below the antenna. As such, these vertical observation wells captured the radial temperature distribution around the antenna.

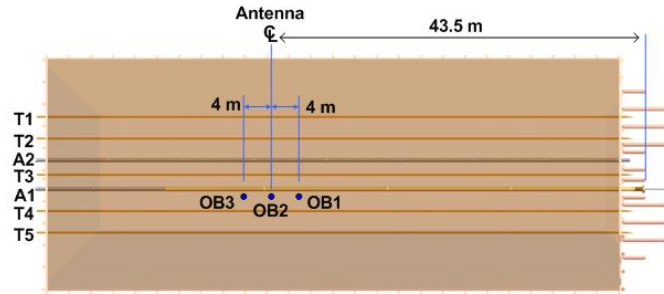


**Figure 8: Aerial view of the layout of the antenna and instrumentation bores for the mine face experiment**

A  $\frac{1}{4}$  wavelength dipole antenna was constructed from 15.2 cm diameter aluminum tubular sections separated by dielectric isolators located at the center feed and tip of the heel section of the dipole. A photo of the antenna prior to installation in the well bore is shown in Figure 9. The linear shape and tubular construction was selected to enable the form factor to be scaled to longer antenna field tests in the future. The modular antenna design could be configured at various lengths between 10 m and 15 m. Electrical measurements prior to the test indicated that a 12.2 m antenna length would provide the best impedance match to the formation over the duration of the test at the intended operating frequency of 6.78 MHz. This frequency was selected because it lies within the industrial band reserved by Industrial Canada for use by industrial equipment. However, there is no restriction on frequency if there is sufficient shielding to surface.

Power was provided from the transmitter to the center feed of the antenna through a copper coaxial transmission line with inner and outer conductor diameters of 3.3 cm and 7.92 cm, respectively. A  $\frac{1}{4}$  wavelength resonant balun was installed adjacent to the heel isolator to prevent stray EM radiation from propagating along the metal tubular back to the mine face. Dry nitrogen was supplied at rates of up to 15 CFM through the inner conductor of the transmission line and exhausted from the Centron casing at the mine face. This provided sufficient cooling for the transmission line.

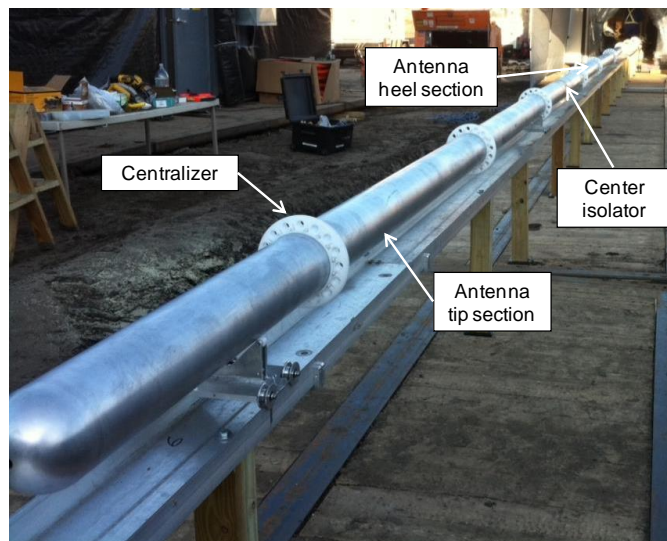


**Figure 9: Installation of the dipole antenna**

The layout of the surface facilities is shown in Figure 10. A 100 kW transmitter provided RF power to the antenna. The transmitter could operate over a frequency range of 4 to 12 MHz. The transmitter shelter provided both heating and cooling so that the transmitter could operate over an external temperature range from -40 C to 40 C. Both temperature extremes were nearly experienced during the operation of the system in Florida during summer and the Dover site in winter conditions.

Operations were conducted from an office trailer that monitored the major subsystems of the test. A nitrogen generation system was housed in a connex and provided the nitrogen supply for the test equipment. A storage connex was used to ship and store the antenna and transmission line components. It also functioned as a work shelter during the construction and installation of the antenna and instrumentation. A 230 kW diesel powered electrical generator and 30 kW backup generator provided power to the site. Communication of the test data and subsystem status was provided by a Harris CAPROCK® self-acquiring trailer mounted VSAT satellite link and permitted real time continuous data monitoring and control of the test to the engineering teams at the Florida and Calgary offices.



**Figure 10: Layout of the surface facilities**

### ***Numerical Model of the Mine Face Test***

The CEMRS model of the test configuration was comprised of three components: the reservoir model, the EM model, and the control software that couples the solvers and defines the electrical material model. Two orthogonal views of the mine face reservoir model are shown in Figure 11. The model domain was 10 m x 15.8 m x 15.8 m (21 x 63 x 63 cells) in the axial, transverse and vertical direction, respectively. For computational efficiency, only half of the antenna and formation was modeled. The symmetry plane was a vertical cut orthogonal to the antenna axis at the center of the antenna dipole. Figure 11 (b) shows the plane of symmetry from the top view at a horizontal plane that coincides with the antenna depth. All

non-symmetry boundaries were modeled as no flow with heat transfer to a semi-infinite body. The location of the antenna is denoted by a white outline. The wellbore was modeled with zero initial oil and water saturation to account for the presence of the nitrogen filled casing surrounding the antenna. Stratification of shale layers around the antenna were included in the model at elevations derived from the core photos and simulated as horizontal layers of low permeability ( $K_h$  from 10 to 100 mD). The shale layers are shown in Figure 10 (a) as well as the reduced horizontal permeability of the sealed vertical observation well (e.g. OB2).

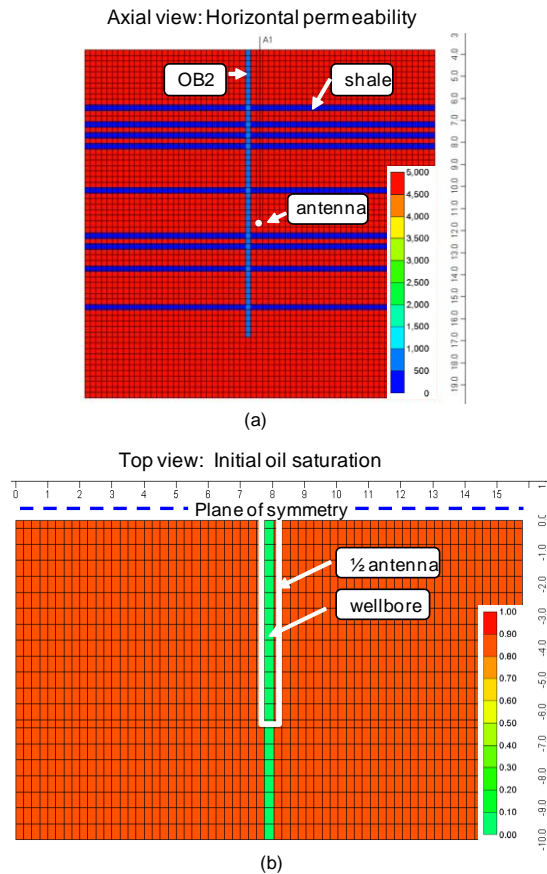


**Figure 11: Reservoir model domain (a) axial view of horizontal permeability, (b) top view of initial oil saturation at the antenna elevation (distance units = m)**

The EM model is shown in Figure 12. The center vertical plane of the antenna was modeled as a symmetric electric field boundary and all other boundaries were modeled as free radiation surfaces. A typical model contained about 140,000 tetrahedral elements. The antenna was modeled with a line source at the center feed and was enveloped by a 10.4 inch (26.4 cm) air cavity created by the casing. Each element in the model received updated electrical properties ( $\epsilon_r$ ,  $\mu$ ) from the material model at every coupling interval. Updates between the reservoir and EM model were controlled by the coupling software and occurred every 0.5 days. Table 1 shows some of the key properties used in the CEMRS model.

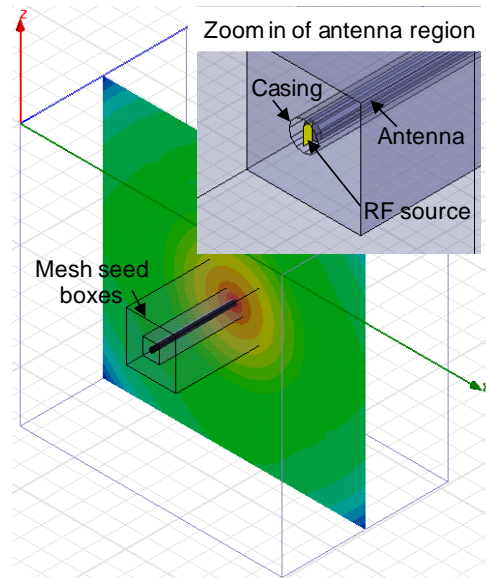
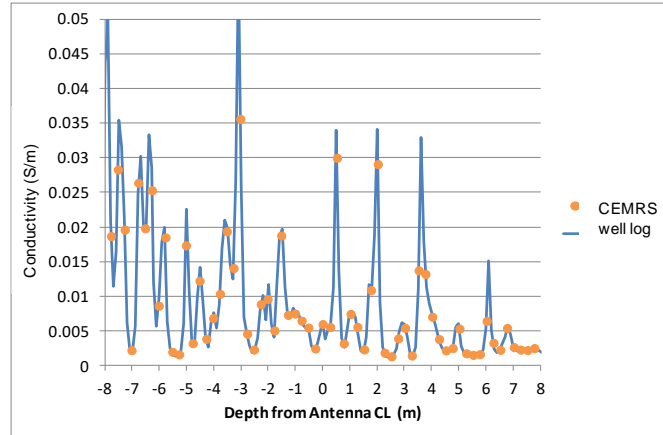


Figure 12: EM model of the antenna and oil sands

Parameter	Value
Porosity	0.31
Average oil saturation	0.81
Average water saturation	0.19
Kh (mD)	5000 in pay 10 to 100 in shale
Kv (mD)	0.6*Kh
Rock heat capacitance (J/m <sup>3</sup> )	2.44E+06
Rock thermal conductivity (J/m-C-d)	751680
Oil thermal conductivity (J/m-C-d)	11500
Water thermal conductivity (J/m-C-d)	53500
Gas thermal conductivity (J/m-C-d)	1400
Thermal conductivity model	Anand
Antenna length (m)	12.25
Antenna OD (m)	0.152
Casing ID (m)	0.247
Initial conductivity (S/m)	Matched to well log

Table 1: Final parameter values used for CEMRS model of the mine face test

To capture the vertical stratification of electrical properties at the test site, the resistivity log from the nearest vertical well was converted to conductivity and the model conductivity was scaled in every cell to match the initial conductivity of the well log along the depth of the model. Figure 13 shows the well log data interpolated onto the CEMRS model. In this graph, the antenna was the datum point at a relative depth = 0 m (~ 11 m below surface). Because permittivity logs were not available, permittivity was estimated based on the water weight of the oil sand [9].

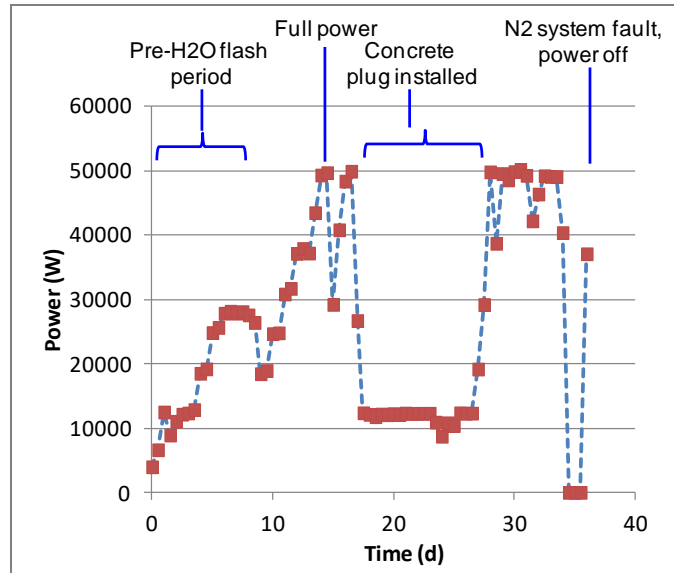


**Figure 13: Conductivity of the formation vs. relative depth from antenna centerline (CL). The antenna is positioned at relative depth 0 m**

### ***Test Results and Discussion***

The mine face test was conducted in three stages. The first stage was a gradual ramp to a low power state of 28 kW that held the formation temperature just under the saturation temperature of water (100 C at 1 atm) in order to collect a data set that preceded the desiccation of the formation. Once desiccation began the electrical properties of the formation would change drastically since water was the primary susceptor of the EM energy. The second stage was designed to ramp to the full design power of 49 kW to observe the effects of desiccation on the radial and axial propagation of the EM fields. The final stage was to turn off the antenna and collect data during the cool down period to better validate the thermal properties of the model.

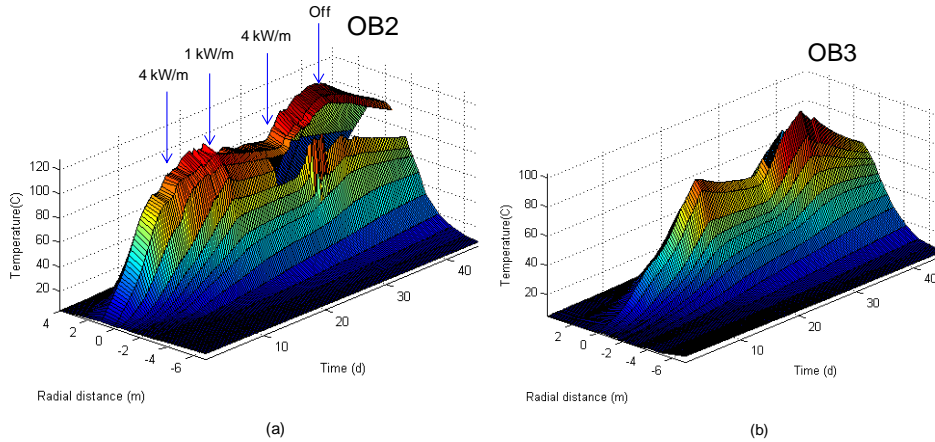
The entire mine face test duration was 11 weeks and included RF equipment setup, the RF heating period, cool down and demobilization. The RF power was initiated on November 20<sup>th</sup>, 2011 and the power schedule shown in Figure 14 was executed. The first stage ramped the power to 28 kW in 6 days and then held to soak the formation at a temperature just below 100 C. After 10 days of low power operation, sufficient data was collected to compare with simulations for the pre-desiccated condition. This was an important test stage because there was little fluid movement and the dominant heat transfer modes were RF radiation and heat conduction. For stage 2 between day 10 and day 14, the power was ramped linearly to the maximum power level of 49 kW, or 4 kW/m for the 12.25 m long antenna. Note that although 4 kW/m was selected as the maximum power density for the mine face test, the antenna was operated extensively at power densities as high as 8 kW/m in extended dry run tests in moist sand at the Florida test site.



**Figure 14: Power schedule provided by the antenna**

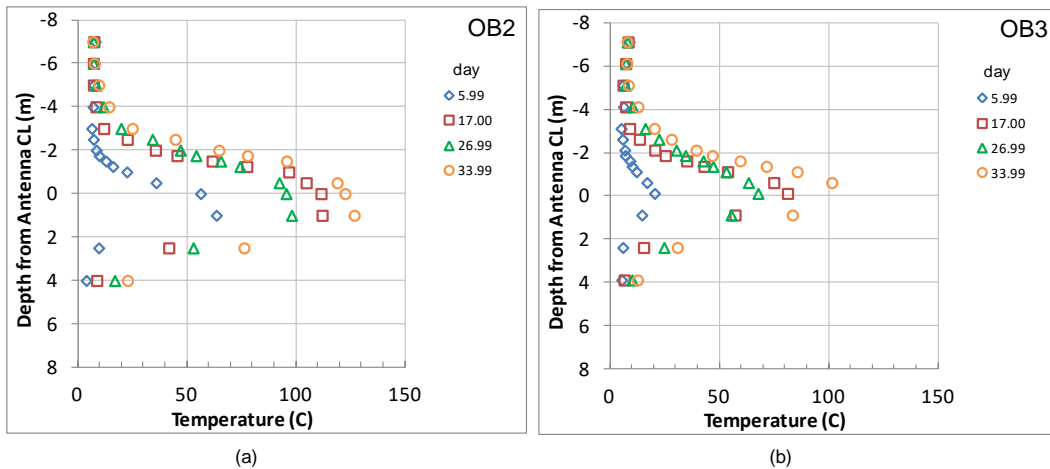
The system was run at 49 kW until day 17. At this time, oil was observed within the annulus formed by the bore hole and casing along the length of the bore up to the mine face. The mobile oil was virtually free of water. In order to avoid any oil drainage at the mine face, the RF power was lowered to 12 kW to maintain formation temperature and a concrete plug with a sampling port was constructed in the annulus at the sand face. This operation took 10 days. Once the concrete was cured, the power was reset to 49 kW and powered almost continuously for 7 days until the middle of day 34. At this time, a connector on the nitrogen generation system was damaged. The connector was repaired and eight hours after the system was restarted the test was terminated due to a failure of the distributed temperature sensor on the A1 bore. Ten additional days of cool down data were collected before disassembling the system. After the casing was removed, it was determined that a thin carbon coating on the distributed fiber self-heated in the RF field. As a result of this finding, the team relied primarily on the discrete optical temperature sensors installed on the OB wells that were confirmed not to self-heat in an RF field.

Figure 15 shows a 3-D composite of the vertical temperature distribution from the discrete fibers on the OB2 (a) and OB3 (b) wells. The radial distance axis is a measure of the vertical distance from the antenna centerline elevation to the sensor position. The plots show how the radial temperature profile in the formation evolved during the test. Figure 15 (a) shows that the temperature along OB2 increased monotonically with time until the power was throttled back to 12 kW on day 17. At this time, the temperature adjacent to the antenna cooled while the temperature at a radial distance of greater than 2 m increased due to continued exposure to RF heating and heat conduction from the relatively warmer center. After the cementing operation concluded on day 27, the power was increased to 49 kW and the temperature at all distances increased until the power was shut off on day 34. During the ensuing cool down period, the central region cooled while the formation at a radial distance greater than 3 m increased by heat conduction from the warmer central region. The empty sectors that appear in Figure 15 (a) after day 20 were attributed to a dropout of two fiber optic sensors. The temperature profiles near the toe of the antenna (OB3) evolved in a similar fashion to those at OB2, but at a lower magnitude with a peak temperature of 100 C observed at that axial location.



**Figure 15: Surface plots of the temperature field evolution at the vertical a) OB2 and b) OB3 wells**

Figure 18 displays the temperature data from OB2 and OB3 on line graphs at several instances during the test. The antenna elevation is represented by the zero coordinate with depth on the ordinate and temperature plotted along the abscissa. The temperature increased throughout the test with the exception of a decrease in temperature at the antenna elevation during the low power operation between day 17 and 27. The maximum formation temperature of 127 C occurred approximately 0.5 m to 1 m below the antenna, not at the antenna centerline. The peak temperature was located at a shale layer below the antenna and confirmed that this higher electrical conductivity material absorbed more RF energy despite a lower RF field strength farther from the antenna.



**Figure 16: Temperature profiles from vertical observation wells a) OB2, b) OB3**

**Numerical Model Results**

The as-tested power profile was input into the baseline CEMRS model that was developed prior to the test. The predictions were compared to the measured data in Figure 17. This represented a blind correlation since the model was not adjusted from the initial settings. The data included the time period from 2 to 20 days, which was generally prior to the flashing of water in the formation. The correlation

was quite good at all times and elevations although the model under predicted the temperature near the antenna elevation (depth 0 m) at the center of the antenna (OB2) by 10 C and over-predicted the temperature at the tip (OB3) by 10 C at day 20.

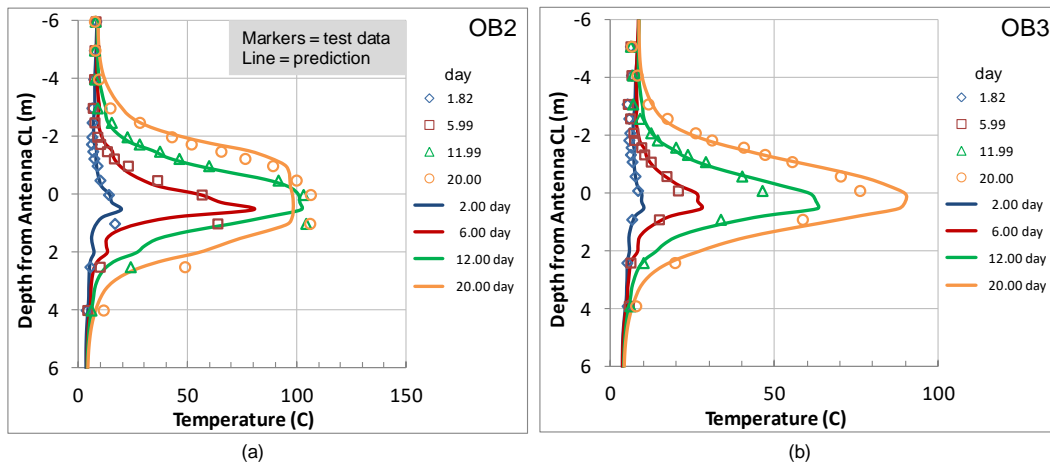


**Figure 17: Comparison of baseline CEMRS model with test data from day 2 to day 20 (a) OB2, (b) OB3**

Figure 18 shows a comparison of the baseline CEMRS predictions with the test data from day 20 to day 43. Again, there was general good correlation along the profile tails. However, during the heating period through day 33 the model predicted lower temperature than the test data at the antenna depth. The simulation showed that water evolved from the high permeability oil sand at 100 C, and at 110 C in the low permeability shale below the antenna.

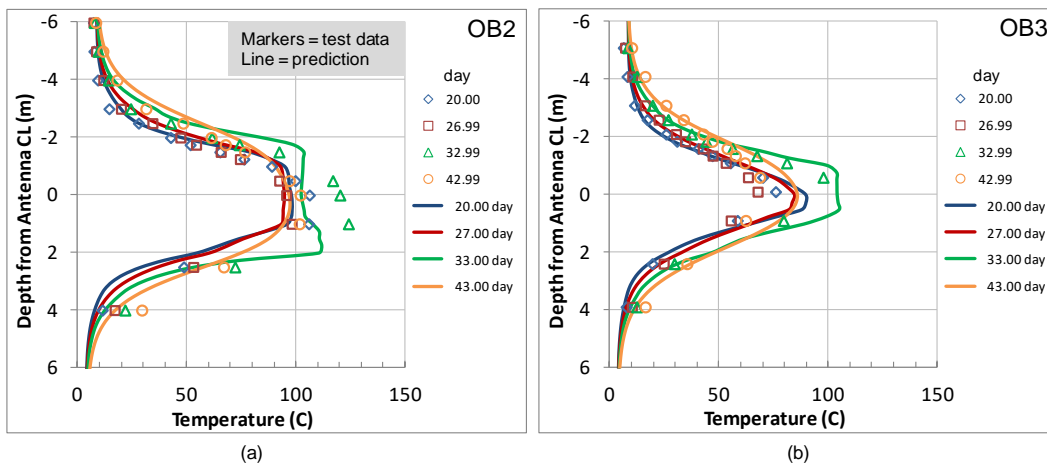


**Figure 18: Comparison of baseline CEMRS model with test data from day 20 to day 43 (a) OB2, (b) OB3**

The shale layers reached temperatures above 100 C, potentially a result of the pore pressure exceeding 1 atm due to fluid thermal expansion in these structures. The model correctly predicted that during the cool down phase (day 33 to 43) the temperature decreased around the antenna, but increased beyond a radius of 2 m from the antenna. This was due to the redistribution of energy by heat conduction since the RF

power was off. The model results at OB3 showed a slower decrease in temperature compared to the test data at this time.

Two changes were made to the baseline model to better history match the data. Firstly, based on observations that the model under predicted the peak temperature in the OB2 profile, the shale layer permeability was adjusted from 60 mD to 10 mD. This change increased the peak pressure and saturation temperature of the water within the shale. Secondly, the baseline model used a simple volumetric mixing rule to determine the bulk thermal conductivity of the formation based on the makeup of the constituent parts (sand, oil, water, gas). This resulted in a small range of thermal conductivity between wet and dry oil sands ( $k_{\text{eff}} = 1.24 \text{ W/m}\cdot\text{C}$  at  $S_w = 0.2$ , and  $k_{\text{eff}} = 1.18 \text{ W/m}\cdot\text{C}$  at  $S_w = 0.0$ ). The cool down data of OB3 suggested that higher thermal conductivity was present at the wet tip because the temperature data decreased faster than the model predictions. However, the data at the desiccated center suggested that less conductivity was required for the model to match the cool down period. A more accurate model of the thermal conductivity of oil sands as a function of water saturation was developed by Somerton [11] and use of this correlation resulted in higher and lower thermal conductivity under wet and dry conditions, respectively ( $k_{\text{eff}} = 1.87 \text{ W/m}\cdot\text{C}$  at  $S_w = 0.2$  and  $k_{\text{eff}} = 0.57 \text{ W/m}$  at  $S_w = 0$ ).

The coefficients of the thermal conductivity model in STARS<sup>®</sup> were tuned to match the Somerton correlation at  $S_w = 0.2$  and  $S_w = 0$ . A comparison of the modified model to the data from day 2 to day 20 is shown in Figure 19. The adjustments did not dramatically change the model results during the pre-desiccation period. The comparison improved near the antenna and at the temperature peak in shale layer just below the antenna.

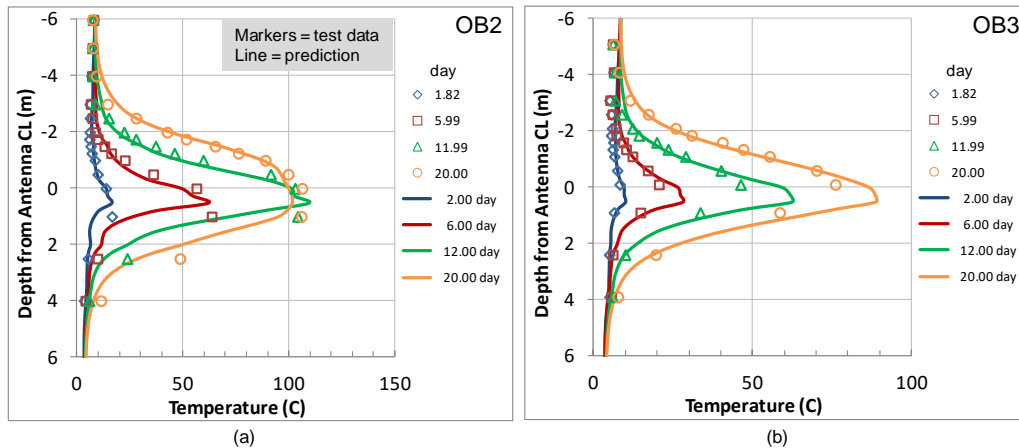


**Figure 19: Comparison of adjusted CEMRS model with test data from day 2 to day 20 (a) OB2, b) OB3**

The result of the modifications was most evident by day 33 day when the formation had actively flashed water for approximately 7 days (see Figure 20). The adjusted model correctly captured the peak temperature observed at OB2, 1 m relative depth, although the model still under predicted the temperature at relative depth 0 to -1 m. Similar results were observed for OB3 at day 33. The predicted temperature decay near the antenna during cool down from day 34 to 43 also improved in the adjusted model. In general, the agreement between the adjusted model and test was quite good, especially given the large variation in applied power during the experiment.

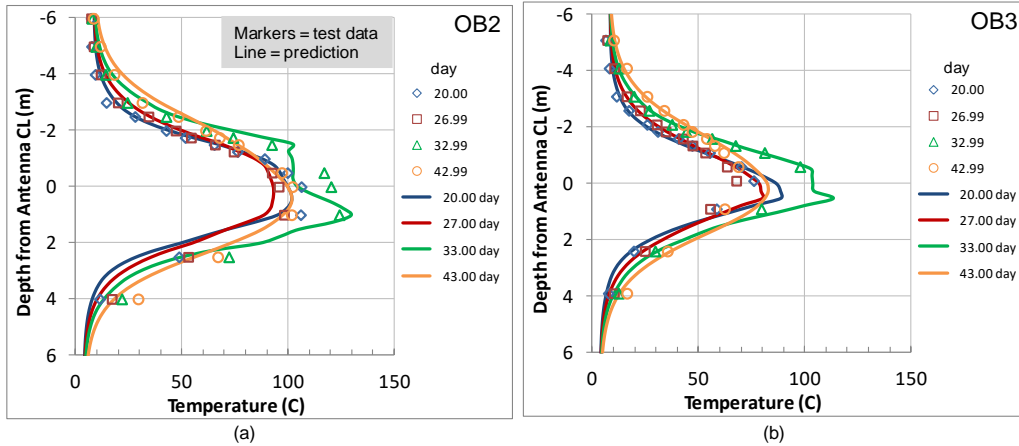


**Figure 20: Comparison of the adjusted CEMRS model with test data from day 20 to day 43 (a) OB2, (b) OB3**

The water saturation was not directly measured during the mine face test. However, the CEMRS model was used to predict the water saturation distribution during the test. The water saturation in an axial plane at the center of the antenna is shown in Figure 21 at day 33. Green contours indicated little to no water saturation within a 1.2 m radius of the antenna at that time. It was noted during the test that water vapor was venting at the mine face and it confirmed that water was removed from the heated zone.

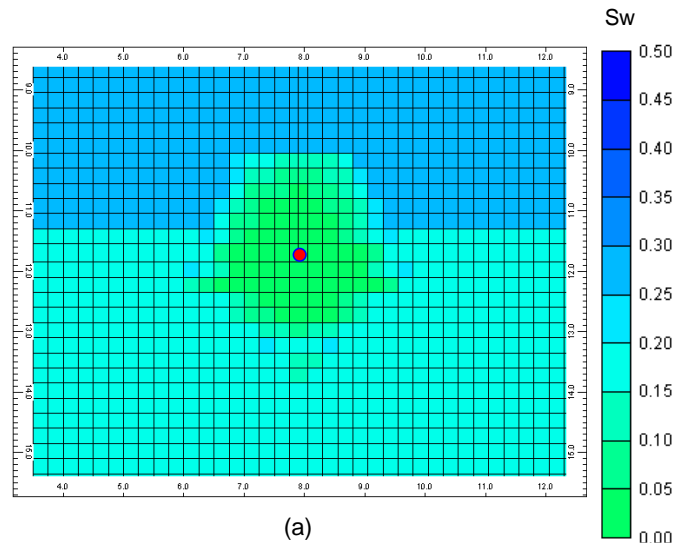


**Figure 21: Predicted water saturation at day 33 from axial view at the antenna center (red dot marks the antenna position, distance units = m)**

The model was also used to predict the temperature distribution as if the test was run at 49 kW (4 kW/m) continuously for 60 days. The maximum temperature achieved was 130 C and occurred under the shale layers directly below the antenna (see Figure 22). The temperature rose to 130 C and 35 C at radii of 2.5 m and 5 m, respectively. Heating above the initial formation temperature extended to a radial distance of 7 m in this time period. The predicted temperature distributions are encouraging for horizontal SAGD

well startup given the typical separation between an injector and producer is 5 m. Configuring both the injector and producer as antennae would significantly accelerate the hydraulic communication between the wells.

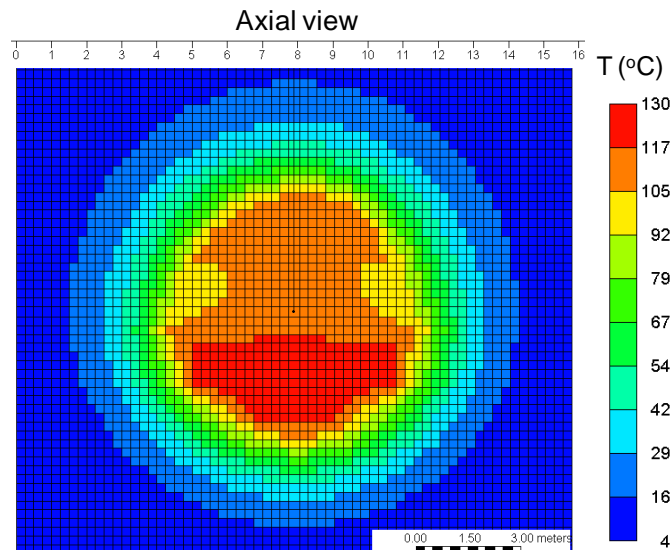


**Figure 22: Projected temperature field after 60 days of 4 kW/m heating at 6.78 MHz from axial view at the antenna center**

### **Conclusions**

The mine face test represented the first phase in demonstrating the ESEIEH<sup>®</sup> process. The primary goals of the Phase 1 project were to demonstrate RF heating of native oil sands at an intermediate scale compared to field implementation and collect a rich data set to validate multi-physics simulations of RF enhanced oil recovery processes. During the program, a modular RF heating antenna was developed that could be configured in lengths from 10 m to 15 m and was tested at 12.25 m. The antenna was inserted into a dielectric horizontal well bore and radiated up to 4 kW/m lineal power density at 6.78 MHz into native oil sands at the Suncor North Steepbank Mine.

A maximum sustained RF power of 49 kW was delivered to the formation and the average power over the 34 day active heating period was 26 kW. The maximum formation temperature observed was 127 C and was recorded on the OB2 instrument string 1 m below the antenna. The peak temperature was located within a shale layer and confirmed the importance of these materials in modeling in-situ RF heating processes in oil sands.

The temperature data collected from the vertical observation wells were compared with predictions from the CEMRS model. Correlation between the test and baseline model was good. The match was improved by decreasing the permeability of the shale layers and by calculating oil sand thermal conductivity based on the correlation developed by Somerton [11].

The history matched model predicted a temperature rise of 130 C and 35 C at radii of 2.5 m and 5 m, respectively, if the system were run at 4 kW/m for 60 days. At these heating rates, the RF system represents a promising technology to reduce the startup period and improve well conformance for SAGD processes, particularly if both the injector and producer are implemented as antennae. It is also worth noting that the RF penetration radius will be significantly larger at commercial antenna lengths of nominally 800 m because of the lower operating frequency.

Despite a shortened operating period, all of the objectives of the mine face test were met. A modular antenna and supporting RF system were designed, manufactured, and installed in a native oil sands test site prepared at the North Steepbank Mine. Robust heating of the oil sands was demonstrated at power levels that were consistent with field level recovery processes in a heterogeneous formation. Furthermore, a comprehensive dataset was collected that validated the CEMRS tool.

### ***Post Test Analyses***

During operations, an accumulation of oil was noted in the borehole. Upon closer examination, the entire bore was flooded with liquid bitumen and audible “gurgling” was recorded. A view down the enlarged bore is shown in Figure 23. Samples were taken from the pool near the borehole entrance for inspection. The produced fluid readily poured. Several samples were sent for analysis and more were stored in refrigeration at site. On 24 December, 2011, one sample was removed for a qualitative pour test. The produced fluids had separated into water and oil portions with the oil above the water indicating an API greater than 10. The sample was then poured into another container as shown in Figure 24. The sample flowed readily at 4.5°C. It was evident that the produced fluid was not the 8 API fluid that was anticipated from the site location.



**Figure 23: View at the borehole entrance accompanied by audible fluid sounds emanating from the opening**



**Figure 24: Sample from the borehole entrance transferred to another container. Sample temperature at the pour time was 4.5°C (40°F)**

After the testing phase was complete, the installed equipment (antenna, casing, instrumentation, etc.) was removed from the mine face in order to continue production operations. The accumulated fluid in the open borehole continued to pour from the open bore as shown in Figure 25 overnight in extremely cold Temperatures.

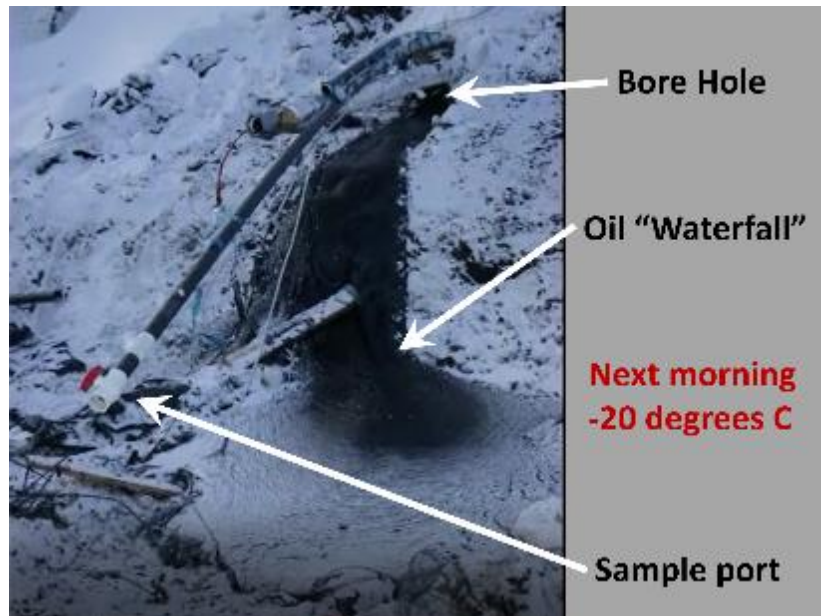


**Figure 25: Sample from the borehole entrance transferred to another container. Sample temperature at the pour time was 4.5°C (40°F)**

Shortly thereafter, the results from the four laboratory samples were received. The results are shown in Figures 25 and 26. There were four samples taken from the mine face test. The produced fluid displayed a clear and consistent shift in viscosity.

- 2000cP at 50C vs. 80C (for typical Athabasca Bitumen)
- 300CP at 80C vs. 110C (for typical Athabasca Bitumen)

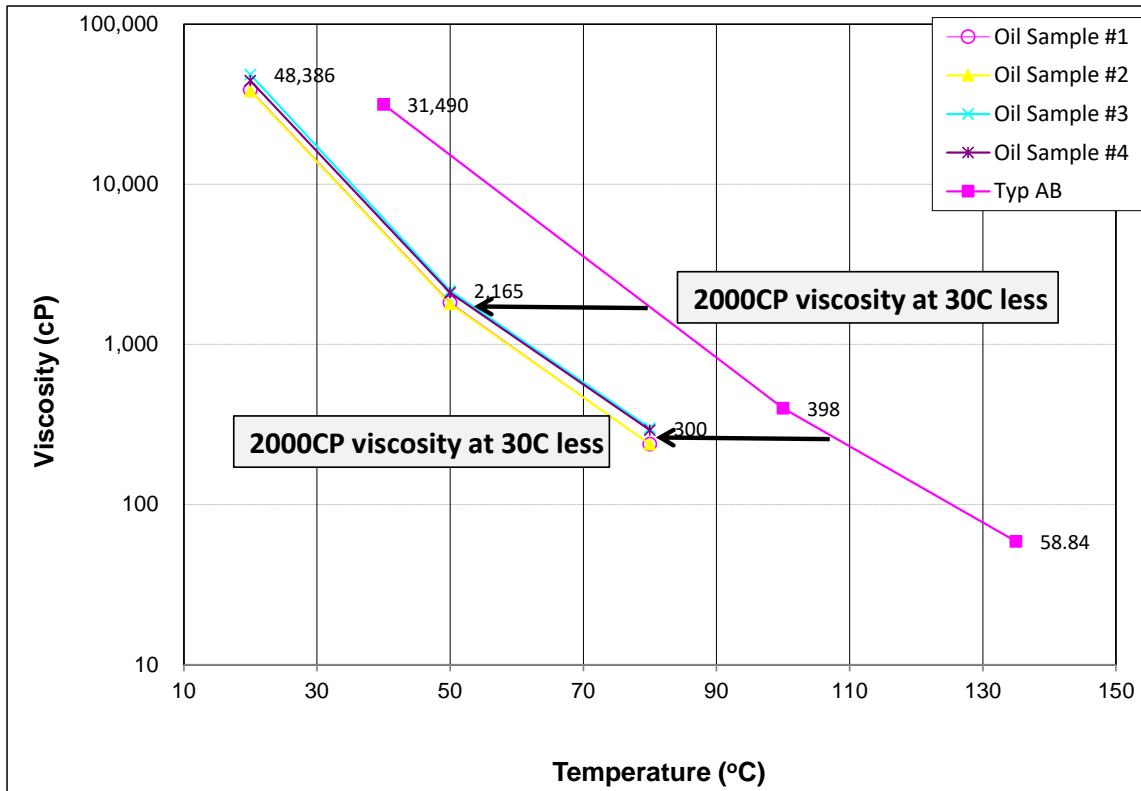
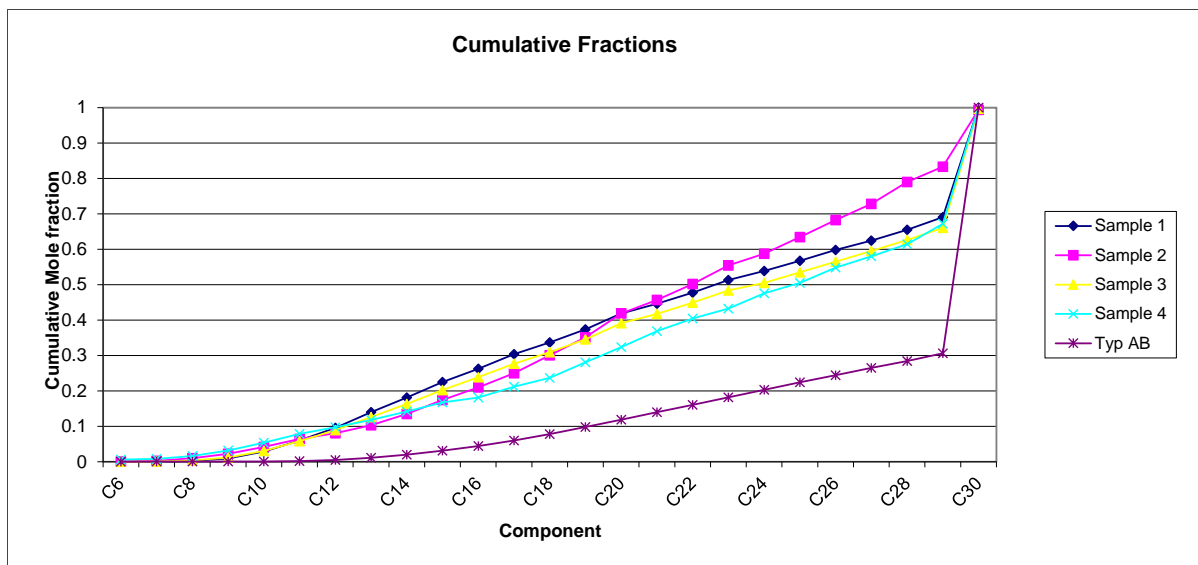


Figure 26: Viscosity of Mine Face Test produced fluid compared to Athabasca Bitumen (Typical)

The composition of the four samples were also tested. As shown in Figure 26, the samples were predominantly below C30 (67-83% vs. 30% for typical Athabasca Bitumen). These results are consistent with the observed flow in the borehole, after the liner removal and in the field pour test.



**Figure 27: Sample compositions from the Mine Face Test produced fluid compared to Athabasca Bitumen (Typical)**

In parallel with the Mine Face Test, outside of the ESEIEH<sup>®</sup> Project, a series of laboratory experiments were performed on the effects of Electromagnetic energy on various types and compositions of oil. There were three phenomena identified:

- **Thermal Separation.** Akin to thermal distillation, constituents are not boiled off. In the Mine Face Test, the reservoir was heated around the borehole to ~100C for a prolonged period of time (higher for a shorter timeframe). This environment mobilized the lighter portions of the fluids which migrated to the borehole where they were collected. The heavier portions were left in-situ as verified via core analysis.
- **Mild Cracking.** There is a significant body of literature investigating cracking with electromagnetic radiation (experimental and analytical). The majority of this work has been in the microwave frequencies yet can be extrapolated to the test frequencies (6.78MHz). A limited amount of laboratory work was conducted in this frequency range that indicated a small degree of cracking. It was demonstrated that frequency does impact the affect results (akin to the Debye frequency for solids). It is unlikely that this phenomenon significantly effected the fluids in the Mine Face test, but discussion is included for completeness.
- The third phenomena were identified via a third-party effort and remains proprietary.

There is an additional factor not present in the Mine Face Test that would come to the fore in an ESIEEH<sup>®</sup> process, Asphaltene Dropout due to solvents. Though not part of this phase, it will become a factor to be considered if/when solvents are coupled with electromagnetic energy.

The potential effects of the combination of these phenomena are unknown and will require further study in the future.

## D. Phase 2 Small Scale (In-situ) Demonstration

### *Introduction*

After a successful Phase 1, the Technical Committee tabling a recommendation to proceed to sanction Phase 2B of the Small Scale Demonstration Test. This review was held following the completion of the detail design work to support an in-situ pilot. Approval was requested to advance detailed engineering, procurement, construction, and test execution with the specific activities being:

- 100 m antenna / injector well
- Production well
- Sufficient instrumentation arrays to collect data and control test
- 2 observation wells + 3 contingent observation wells
- Surface facilities, control system and infrastructure
- Operations for 7 month test period
- G&G interpretations and geo-modeling
- Reservoir recovery modeling and correlation w/ field data
- EMH system technology development; transmitter, transmission line (surface and sub-surface), antenna, test procedure CONOPS
- Data management
- Decommissioning & reclamation

Phase 2 objectives were defined as follows:

1. Demonstrate and measure bitumen drainage due to RF heating and propane vapour – empirical test.
2. Measure other key economic indicators including solvent retention, power consumption and delivery efficiency of EM energy to the reservoir.
3. Test the sensitivity of drainage to operating conditions such as power, solvent injection rate or pressure, production rate controls etc.
4. Provide field data to guide predictive numerical modeling and optimization.
5. Determine the behavior and disposition of solution methane under ESEIEH® conditions.
6. Pilot ESEIEH® RF hardware and well design with respect to functionality, reliability and efficiency.

Immediately following the review, Laricina withdrew from the project. As a result, partner sanctioning of the project was deferred pending successful negotiations with Devon to enter the consortium. Suncor and Harris continued to advance the project work with full Integrated Project Team (IPT) engagement on the expectation that partner sanction would be ratified by the end of the year.

Partner technical assurance reviews proceeded through the fall and amended partner agreements were executed in January 2014. Full partner sanction was received April 2014. Following partner sanction, the project scope was expanded to include:

- An additional observation well
- An additional 17-month test period

### ***Test Site***

Suncor's Dover site (Township 93 Range 4 W4) was picked to host the Phase II pilot for a variety of reasons: good to excellent reservoir quality, well understood geology, and close proximity to Suncor's MacKay River operation. Dover is famous as being the birthplace of SAGD with the Underground Test Facility (UTF) being directly beside the selected ESEIEH® site which was once used for the Vapor Extraction (VAPEX) pilot (see Figure 28).

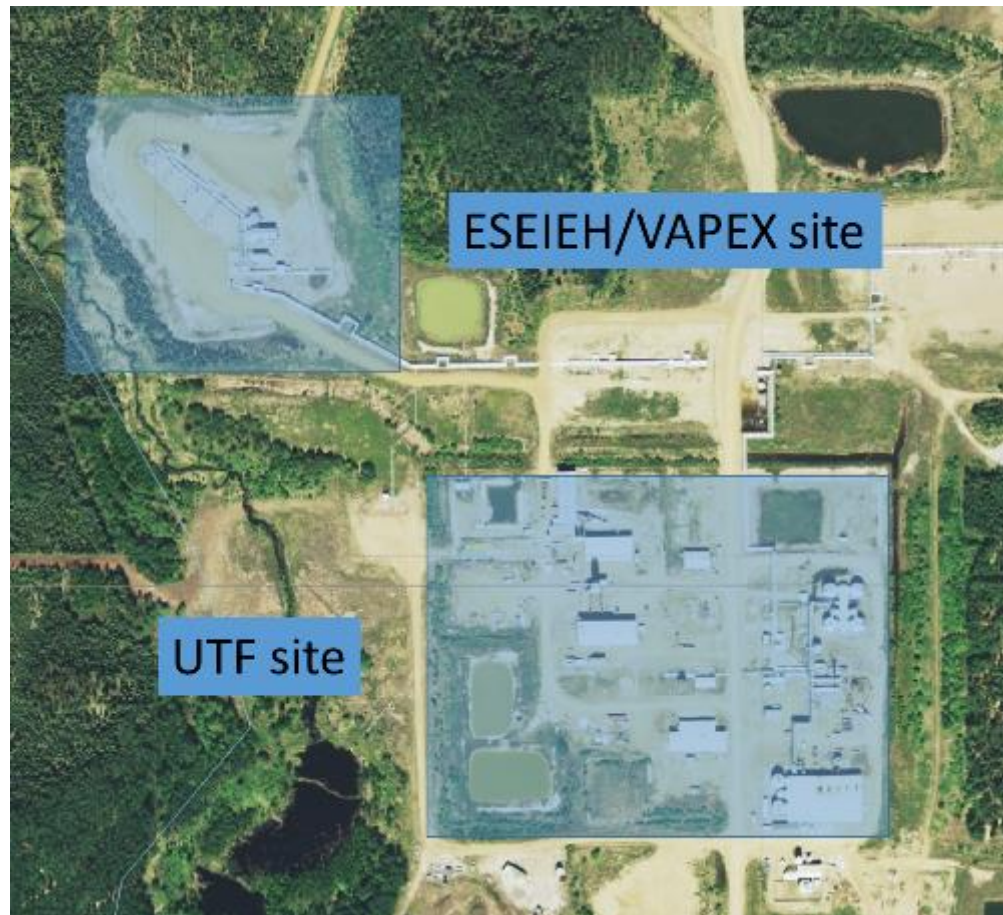


**Figure 28: ESEIEH® Test Site**

### ***Well Design***

The antenna/injector well design (EZI-1) was a synthesis of the Phase 1 antenna, and a standard SAGD injector with multiple design enhancements (see Figure 29).

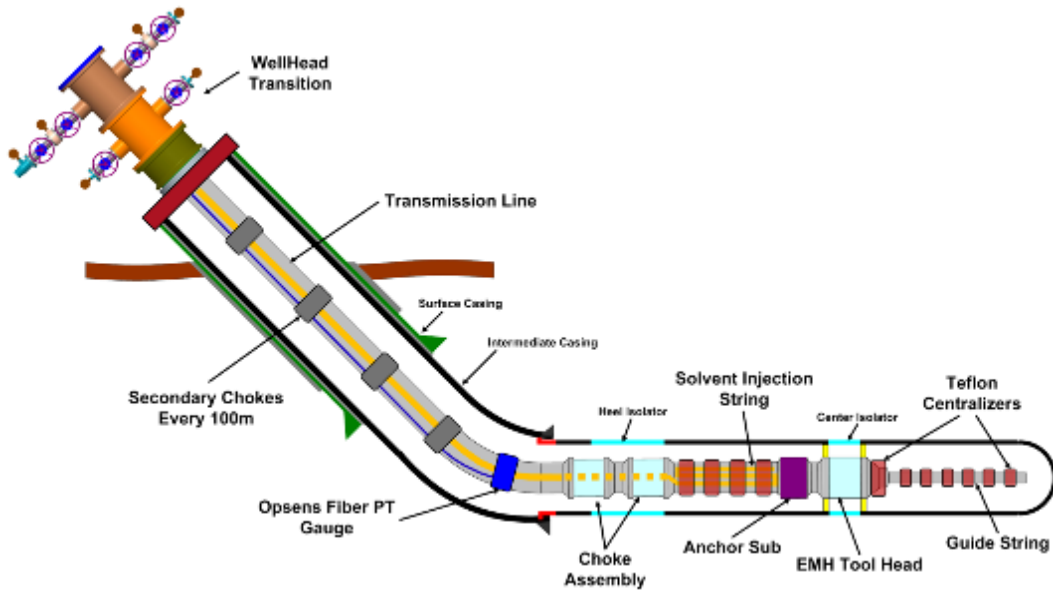


Figure 29: ESEIEH® Phase II Antenna/Injector (EZI-1)

The Producer well (EZP-1) was run with a standard slotted liner and a progressive cavity pump (PCP) for artificial lift. Three observation wells were drilled with RF transparent casing, pressure and distributed temperature sensors.

Following the design and fabrication of a ‘prototype’ antenna, a handling test was successfully completed as a pre-gate activity (see Figure 30). The purpose of the test was to provide training to Suncor’s designated completion rig contractor and crew, and to test equipment interfaces and tool handling capabilities.



Figure 30: Handling Test

**Well Placement**

The 100m horizontal wells were drilled in 2014 between the 2 VAPEX well pairs at a 50m standoff. Calculations showed that the reservoir at this location would be unaffected by the VAPEX vapor chamber. Two observation wells (EZOB-1, EZOB-2) were drilled at the center of the antenna/injector and one (EZOB-6) at the heel for data collection (see Figure 31). The Producer was drilled in clean bitumen at ~279m TVD SS with the injector drilled at 284m TVD SS (see Figure 32).



Figure 31: Well Placements

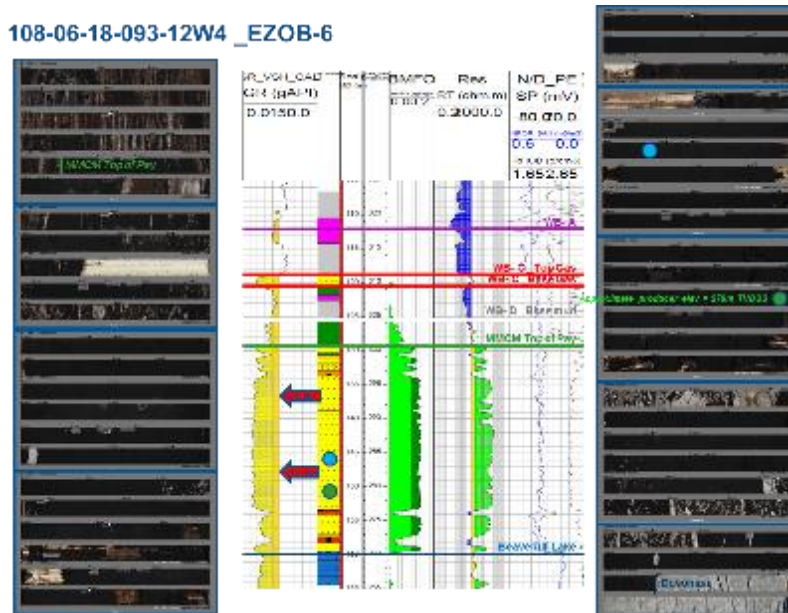


Figure 32: EZOB-6 Core and Well Pair Placements

### ***Coupled Electromagnetic Reservoir Simulator (CEMRS)***

During the early period of phase II of the CCEMC project Harris worked closely with Laricina to conduct initial simulations of the ESEIEH<sup>®</sup> recovery process. The models have since expanded significantly through joint engagement with all current project partners. The model of the Dover site was updated in three stages; the first model was a 2-D domain based on course reservoir descriptions and well logs. This model was updated with more detailed reservoir descriptions from Suncor geologists and the electrical properties were matched to surrounding well logs, and a 3D model of the test site was constructed by extruding the updated 2-D model along the axis of the antenna.

The initial 2-D model was used to conduct a survey of candidate RF power profiles that could be applied during the test. The antenna was always operated at the highest power (4 kW/m) for the first 60 to 90 days in order to promote timely hydraulic connection between the injector and the producer. After communication was established the RF power was reduced and it was found that the oil rate reduced less than linearly with the sustaining power. Given this, a nominal sustaining power of 1 kW/m was proposed for the test in order to promote an energy efficient recovery process. A detailed study was conducted to evaluate the effects of linear, exponential and cyclic sustaining powers. It was found that a linearly decreasing power profile maximizes the oil rate. The study also concluded that methane accumulation within the formation may occur as a result of liberation of the dissolved methane in the native bitumen. The sustaining solvent injection rate was predicted to be ~ 1000 kg/day with a maximum usage of 2500 kg/day recommended for facility design. It was determined that the solvent usage was reduced by limiting the bottom hole gas volume produced from the producer.

3D simulations revealed that the antenna in direct electrical contact with the formation heats initially in a localized region around the center of the antenna, but as the formation desiccated the heating broadened to encompass the entire axial length of the antenna within approximately 45 days. It was found that propane could be injected after a 60 day period, although heating at full power of 4 kW/m for 90 days was recommended. It was also found that, as expected, higher RF frequency (4 MHz) had an initially more compact heating pattern around the center of the antenna compared to lower frequency (900 kHz), but both showed successful startup of the ESEIEH<sup>®</sup> process over the same time periods. A comparison of 2D and 3D simulations showed that the fluid injection and production rates for the 2D model were similar to those predicted by the 3D simulation and therefore the 2D model should be valid to use to establish trends and sensitivities of process rates.

A detailed survey of the frequency dependence of the VSWR was conducted for a family of transmitter bandwidths and it was determined that the best frequency range for the Dover test was 800 kHz to 4 MHz. The simulations revealed that most of the frequency variation required for the test occurred prior to the desiccation zone enveloping the antenna. Once this stage was reached the sustaining operating frequency was quite stable at approximately 1.2 MHz.

A study was conducted to evaluate the short term and long term benefit of installing a small heater (not RF) at the producer. Doing this caused the entire length of inter-well region and producer to be heated to > 100 C within 90 days. The oil volume drained was larger after 90 days compared to the baseline configuration with no producer heater, but the differences decreased at later times, with little noticeable difference after 2 yrs of operation.

## Facilities

The final design of the ESEIEH<sup>®</sup> surface facilities consist of six major components (see Figure 33):

- (i) Transmitter House or T-house – Houses the 500kW transmitter and instrumentation that supplies the RF power downhole
- (ii) Dielectric Fluid Conditioning System (DFCS) House or D-House – Houses the DFCS which provides capability to condition and cool the dielectric fluid used to cool the antenna's chokes.
- (iii) Separator Building/Flare - The separator building contains the production handling capabilities for the pilot. This was an original VAPEX facility which was 'repurposed' for the pilot.
- (iv) Product Storage Tank - The Product Storage Tanks is a skid-mount 10'x30' 400 bbl vessel complete with off-loading pumps and metering facilities.
- (v) Solvent Storage Tank - The Solvent Storage Tanks is a skid-mounted vessel complete with product loading/metering facilities responsible for containing propane solvent for process injection
- (vi) MCC Building - The MCC Building houses all the control units to support the pilot operations (common power bus, programmable controllers, metering, communications, etc.) This was an original VAPEX facility which was 'repurposed' for the pilot.

Field Construction started in September 2014 and was finished in May 2015. Commissioning took place immediately after with the systems being ready for start-up on July 9<sup>th</sup>.

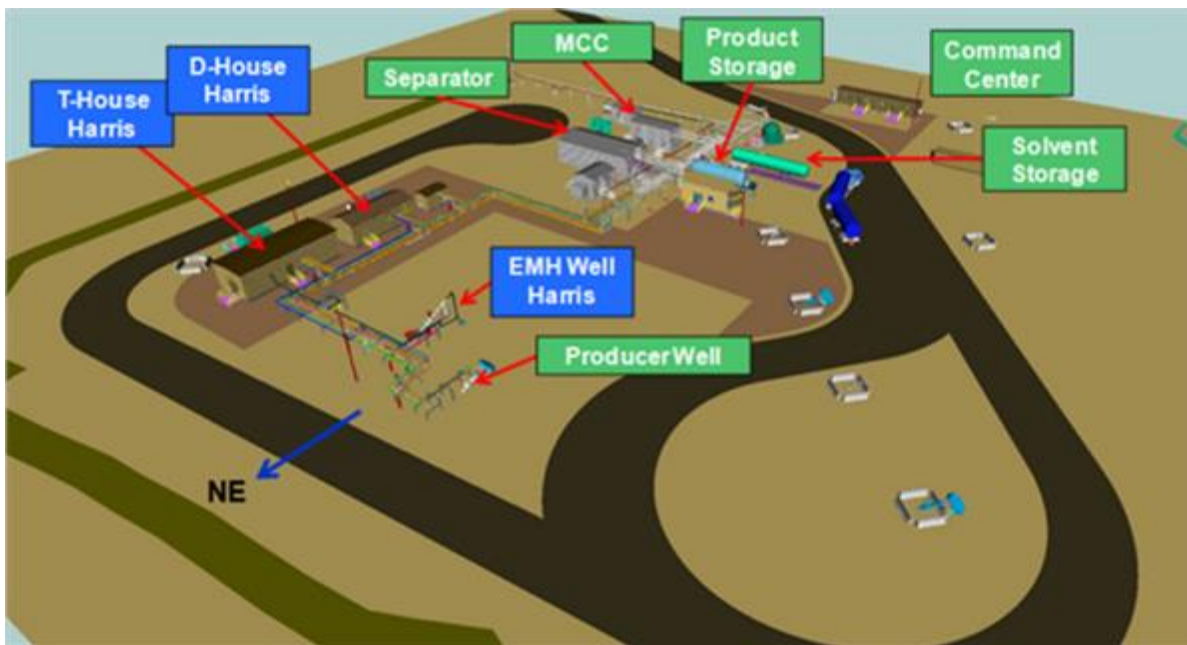
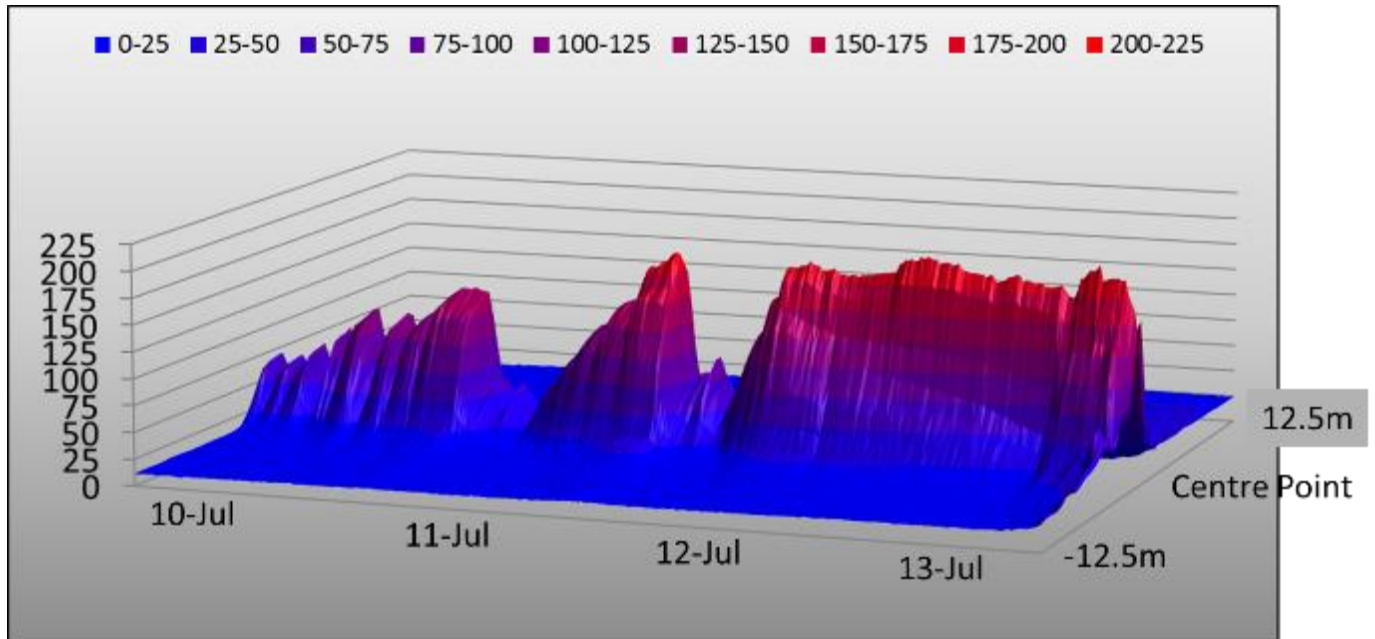


Figure 33: ESEIEH<sup>®</sup> Small Scale Pilot Facilities

### Pilot Operations

The pilot test plan was officially executed on the morning of July 9, 2015. Throughout the next days the power was raised as per the operating plan. Minus the minimal downtime on July 11<sup>th</sup> and 12<sup>th</sup> the reservoir was heating up as expected (see Figure 34)



**Figure 34: Start-up Temperature Profiles in degrees Celsius (Center Point)**

A significant VSWR event occurred on 1645hrs on July 13 which resulted in power shut down and an observed rapid temperature drop from 180 to 60 degrees C. Harris concluded that the VSWR trip was likely due to a set up issue and that the fast cool down may have been caused by rapid influx of cool water to the feed area following power shut down. Operations were immediately suspended to conduct an investigation.

A series of N<sub>2</sub>/diesel displacement operations were conducted on EZI-1 to determine the effect of fluid displacement within the lateral on antenna impedance. These displacements were conducted under low power on July 26 and 27. The concept was to generate some local convective heating in an effort to displace high conductive fluid away from the tool head. The displacement operations indicated only a minor impact on downhole impedance. Continue with low power (10 kW) throughout the period of suspended operations in an effort to maintain minimal downhole heating.

Operations completed a series of N<sub>2</sub>, N<sub>2</sub>/diesel and dilbit displacement throughout August with some indications of improved downhole conditions. Operations also identified and resolved a transmitter cooler water leak during the same time period.

A second unsuccessful attempt was made to deliver high power to the downhole assembly in early September.

After developing revised procedures for 'high power' restart and recalibrating all the surface instrumentation and sensors, an attempt was made in early September to re-established peak power while staying within pressure and temperature limits. The tool appeared to enter within boiling

temperature range approximately 45 minutes after start-up with the transmitter shutting down in response to abrupt impedance change. Following an immediate restart, the VSWR continued to decrease indicating that desiccation was likely taking place, however downhole temperature limits were exceeded and the test was suspended. Harris concluded that the transmitter shutdown was a 'false positive' response as a result of faulty attenuator pads. As a result, a number of operational recommendations were made in attempts to mitigate future shut-downs.

A dilbit displacement & high power start-up was again attempted on EZI-1 in late September with no measurable improvement in downhole impedance. Operations continued to operate through October 2015 at reduced power at steady state temperature, however were unable to increase power.

Following further surface modifications to increase the safety margin of both the IOB and STL, the transmitter was returned to service in early November. While running at ~70 kW, a significant VSWR shift was observed indicating a possible arcing event and the transmitter was immediately shut down. A subsequent restart indicated high harmonic content along with a 'lower explosive limit (LEL)' alarm on the DFCS return indicating high heat. As no heat was observed downhole, it appeared that the location of the short was within the IOB.

The EZI-1 wellhead inspection was completed in mid-November 2015 and confirmed that the N2 Barrier is damaged and will have to be replaced. The damage appeared to be caused by an arcing event. Metal debris was present. The contamination was very high and likely the source of the voltage breakdown. The IOB was removed and shipped to Harris in Florida. An inspection of the surface facilities identified significant metal debris in the surface lines and thermal accumulator vessel. It was determined at that time that the antenna was non-operational.

Operations were suspended on December 9, 2015. The antenna was extracted from the well in March 2016 in support of the failure investigation.

## **E. Phase 3 Restart**

### ***Phase 2 Investigation***

Following the suspension of the Phase 3 Operations, the ESEIEH® Technical and Management Committees concluded that a (i) formal technical investigation, (ii) Root Cause Analysis (RCA) (iii) and a formal gate review would be conducted prior to the project moving forward (Phase 3 Restart). An investigation team was established to collect key evidence in support a formal RCA.

A Root Cause Analysis session was convened with a scope that included (i) developing a 'sequence of event' chart leading to the failure(s), (ii) defining causal factors, (iii) facilitating a root cause analysis on each causal factor, and (iv) facilitating the development of a corrective action plan.

The primary causal factors for this incident were determined to be the presence of external rust and foreign objects/debris ("FOD") from intermediate casing pushed into tool head isolator. These causal factors were likely a result of remediation procedures during the initial completion which introduced metal FOD and rust downhole, resulting in the initial failure of the antenna by causing the center tool head isolator section to overheat and fail.

The root cause of the failure was identified as a combination of technical and quality controls issues that occurred during the project execution. The root cause analysis identified several corrective actions to improve ESEIEH® processes and design to prevent a recurrence in the next phase of operations.

In response to the RCA outcomes, work was immediately undertaken to investigate alternative configurations for remediation of EZ I1. Initial study work was led by Suncor under close collaboration with Harris, Suncor Drilling & Completions. This work was supported by detailed design work which included both detailed electrical analysis and numerical modeling.

**Phase 3 Redesign Activities**

In August 2016, a selection (*i.e. restart Option 1a*) was made supporting a mono-bore horizontal antenna well configured with a dedicated vertical solvent well (see Figure 35). The ‘mono-bore’ design provides the best opportunity to ensure an optimal operating environment for the antenna. Unfortunately, the existing intermediate casing did not allow for the integration of solvent injection, therefore a separate vertical solvent well was required to meet the overall testing objectives. This recommendation was supported by significant modeling work to assess impacts on the coupled recovery process.

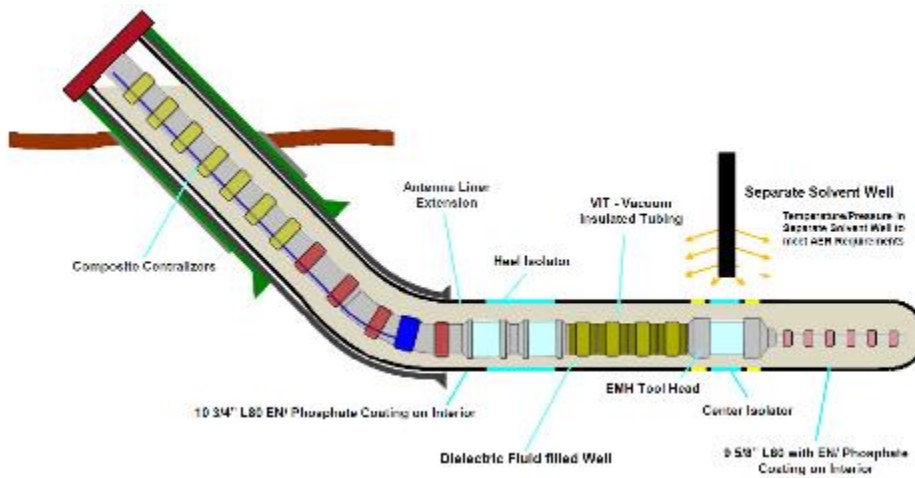


**Figure 35: Revised Design - ESEIEH® Phase II Antenna/Injector (EZI-1)**

The surface facility was modified to adapt to the vertical solvent configuration (see Fig 36). Project sanction for Phase 3 Restart was awarded by the partnership in July 2017.

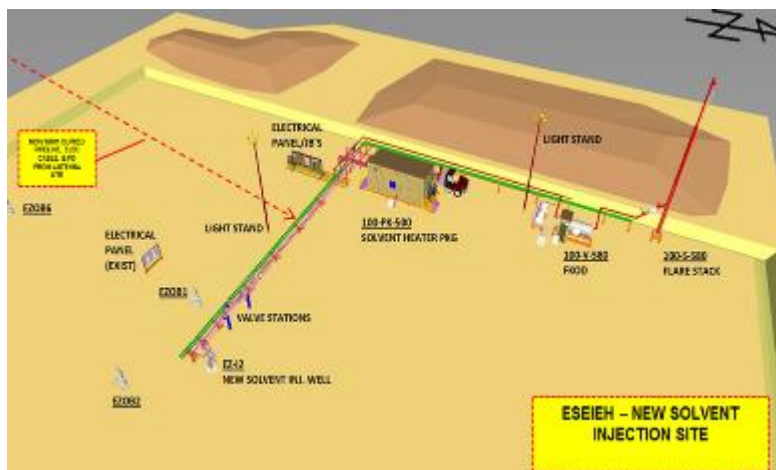


**Figure 36: Revised Design - ESEIEH® Phase II Solvent Injection Site (EZI-2)**

Summary of Mail Ballot 2018-02S (Full supporting RCA report is in attachment [ESEIEH RCA 2018 Technical Committee Rev2\\_0](#))

Detailed redesign work continued through 2017. In November of 2017 a second attempt to run a redesigned sealed monobore antenna liner failed when it became lodged within the intermediate casing. A second RCA identified that the isolator OD clearance was too tight and allowed to flex in non-optimal locations with respect to the intermediate casing ID and high dogleg tight spots. In addition, hole cleaning operations prior to the antenna run-in-hole (RIH) were not sufficient to ensure that the relatively tight wellbore was unobstructed with bitumen/sand/FOD.

During the first half of 2018 the isolator assembly has been redesigned following significant running clearance analysis as well as torque and drag modeling of the final accepted assembly. These works were commissioned to ensure that the monobore antenna liner assembly can successfully be landed as designed without damage. This includes significant re-work of the programmed running procedures to ensure that the actual observed running loads are both understood and adhered to ensure that the assembly is not subject to running conditions that would result in sticking and/or breaking the assembly.

Most importantly, the two RCA's highlighted that previous operations within the EZ-I1 wellbore have impacted the wellbore integrity and leave opportunity for the presence of conductive metallic FOD. The antenna liner running program has been extensively re-worked to include active, pressure induced hole cleaning operations that utilize a forward circulation venturi system, magnets and junk baskets. This equipment and the incremental cleaning/evaluation procedures allow more definitive FOD collection and evaluation than possible in 2017.

A memory logging tool will also be run during open-hole cleaning operations to evaluate the impact on open-hole conductivity due to the presence and recovery of conductive metallic FOD. This same tool was utilized during the initial EZ-I1 hole drilling and thus provides a baseline for run-to-run comparison as the wellbore cleaning runs are carried out. The run-to-run observed results will be evaluated against baseline FOD contamination tests run at both Harris and the logging tool service that has validated this tool and procedure.

The execution of Re-start Option 1a (High Power Start-up) or Option 1b (Low Power Start-up) are contingent upon a positive acceptance of the EZ-I1 open-hole conductive FOD assessment.

The CCEMC Pilot low power checkout was successfully completed on December 21. This demonstrated the operation of surface and subsurface equipment from the PCS by on site personnel through a planned transmission of approximately 5kW of power at 1.7MHz through the EMH tool and into the antenna for a duration of 15 minutes.

CCEMC MPR 094 (Jan 2019)

Figure 37 summarizes the completion schedule for the major Phase 2b Re-Start project items that have been executed since the EZ-I1 open-hole clean-out and evaluation in September of 2018 leading to RF Start-up.

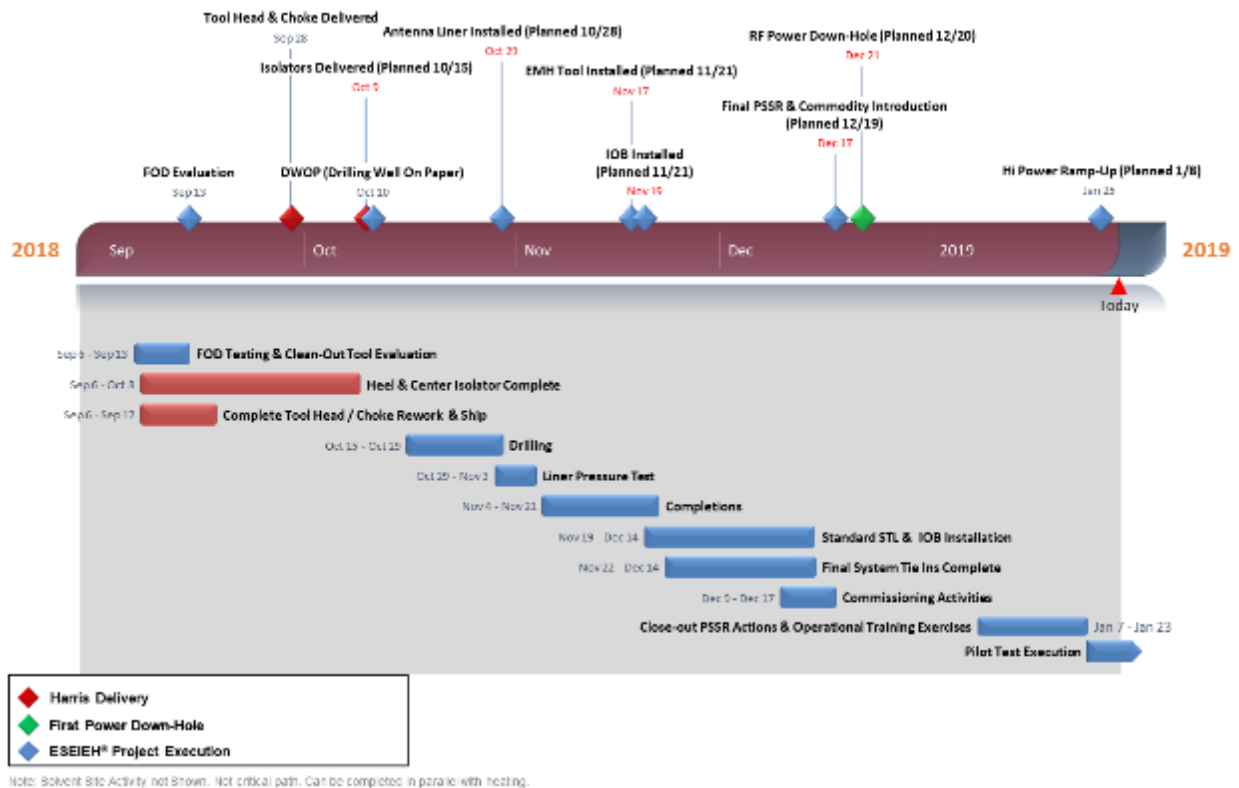


**Figure 37: Revised Schedule from Jan 2019 MPR**

Pilot RF start-up occurred on January 25<sup>th</sup>, 2019, a significant project milestone. A series of power off test was planned to measure thermal decay in the reservoir and validate the CEMRS model of the system. The performed power profile is also shown. The planned power ramp-up schedule as shown below could not be completed as intended due to an onset of a Voltage Standing Wave Ratio (VSWR) event which occurred on February 20<sup>th</sup>, 2019 at still relatively low power levels. This is indicative of an

anomalous electrical circuit problem within the RF delivery system (Reference: CCEMC MPR 095 - Feb 2019).

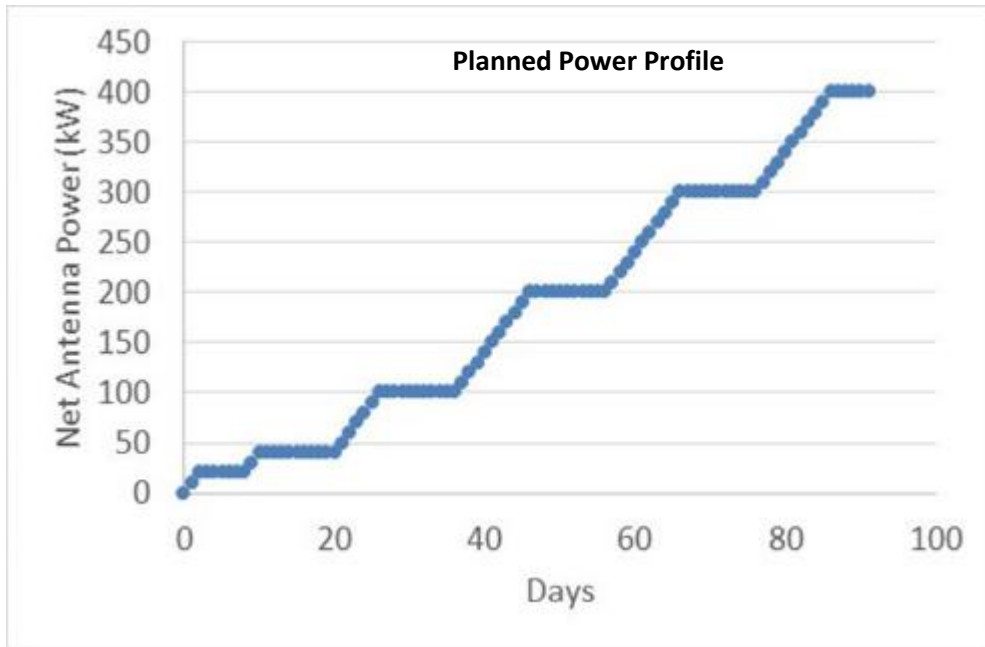


Figure 38: Planned Restart Power Ramp from Jan 2019 MPR

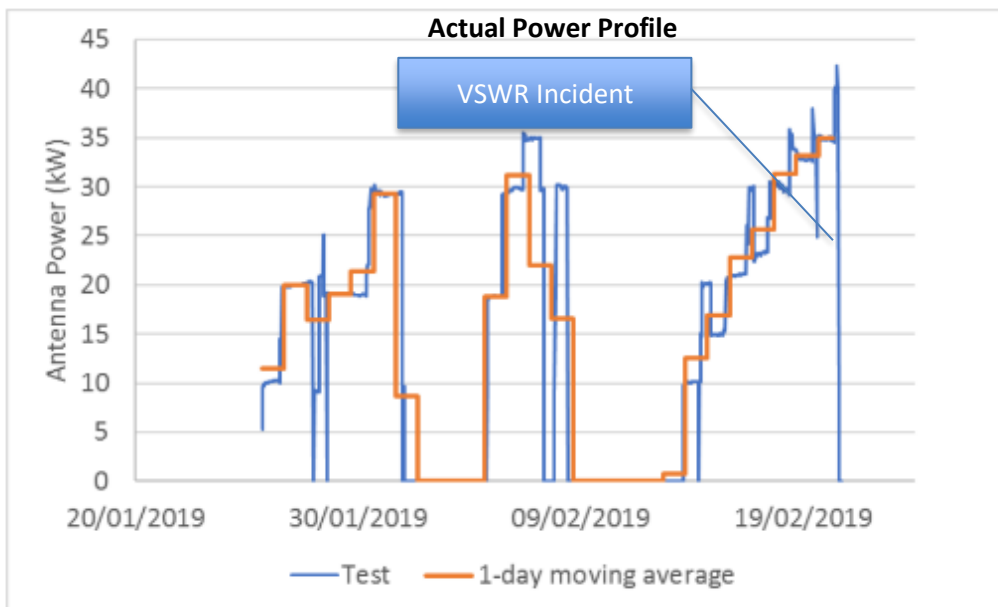


Figure 39: Actual Power Profile from 2019 Restart

Troubleshooting determined that the transmitter can no longer be reliably run without risking further component damage, and the electrical short or circuit problem is most likely to be within the downhole components. At this point, RF cumulative uptime was only 16.9 days (65%). Temperature profiles through the anomaly are shown below. It should be noted that with an average power of 1.5KW/M input energy (<40KW maximum power), heating was observed at the producer 5 meters away with only 17 days operation. This measurement was confirmed by the observation well data.

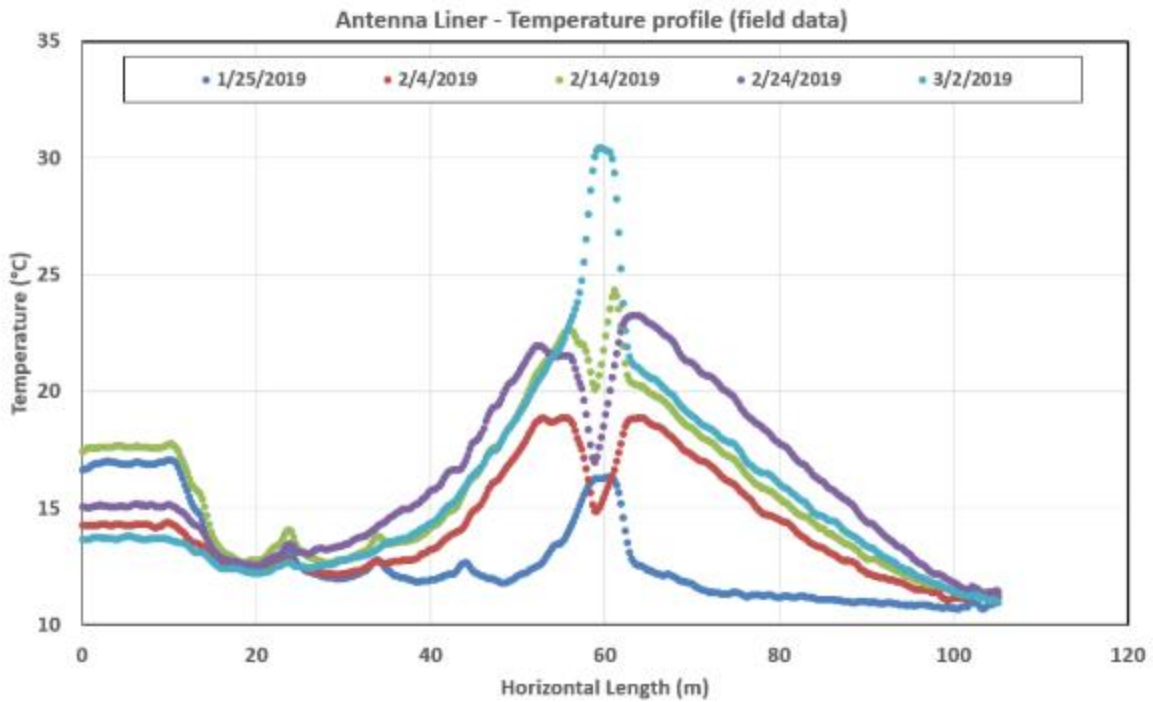


Figure 40: Liner Temperature Profile 2019 Restart

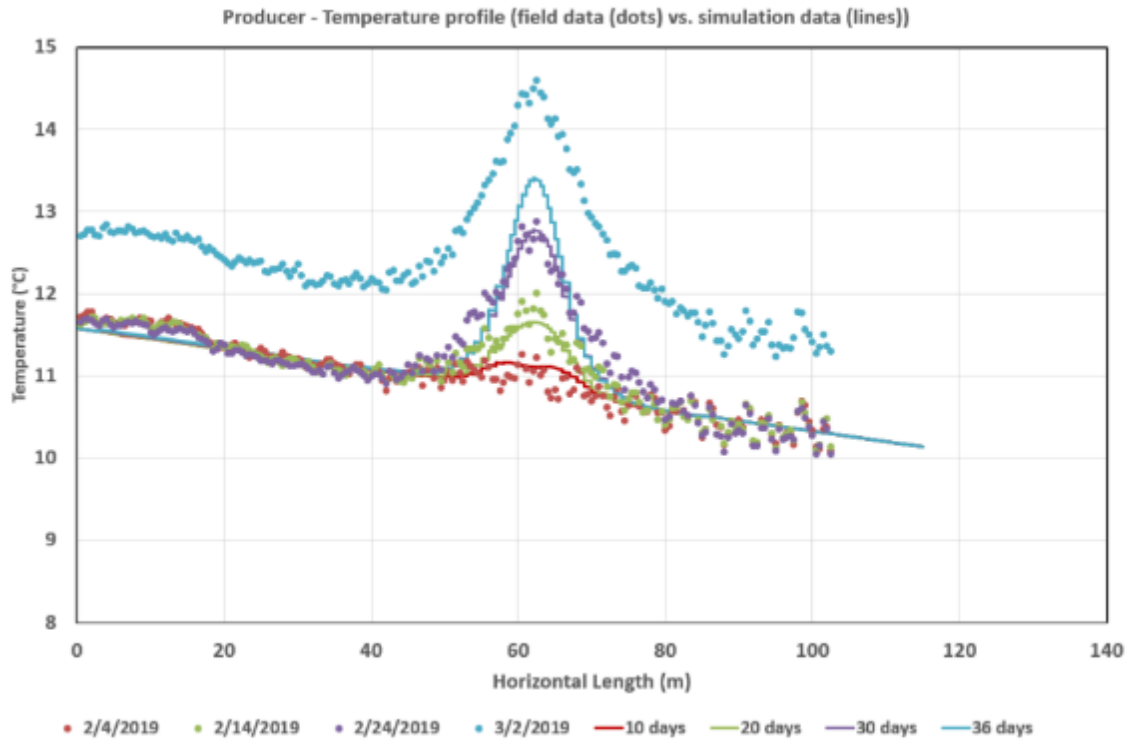
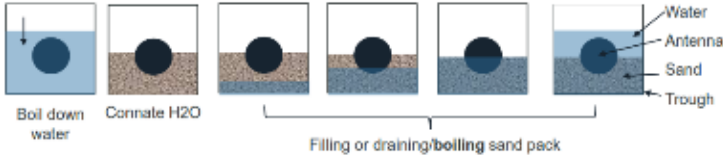


Figure 41: Producer Temperature Profile from 2019 Restart

**RCA**

A timeline of the key 2019 activities to recover the downhole equipment and determine root cause is outlined below. Full technical details may be found in the attachment ([20191014 ESEIEH Low Power RCA Failure Replication Report](#)).

Activity	Date	Findings
Pull the Inner Completion	April 2019	<ul style="list-style-type: none"> <li>No damage found in the EMH toolhead. Function checks OK</li> <li>Camera run inside the liner and no indication of significant wellbore fluid contamination</li> <li>Materials sample analysis completed</li> </ul>
Plan for offsite scaled testing	May 2019	<ul style="list-style-type: none"> <li>Build the above-ground, tank apparatus in Florida. Connect to transmitter designed for full-power equivalent</li> <li>Started to procure scaled prototypes of the as-built liner section. Highly likely that this is the point of damage</li> </ul>
Execute Scaled Testing Plan	June 2019	<ul style="list-style-type: none"> <li>Finalize design of scaled test articles and test fixtures</li> <li>Begin <i>failure</i> replication phase Hi pot testing</li> </ul>
Execute Scaled Testing Plan,	July 2019	<ul style="list-style-type: none"> <li>Continue <i>failure</i> Hi pot testing and begin submerged testing (sequence of steps illustrated below)</li> </ul>

<p>Pull Liner</p>		 <ul style="list-style-type: none"> <li>• Pull liner. Inspect exterior damage. Ship to Florida for detailed RCA</li> <li>• Begin to procure <i>mitigated</i> design prototypes</li> </ul>
<p>Execute Scaled Testing Plan,</p>	<p>August 2019</p>	<ul style="list-style-type: none"> <li>• Complete all <i>failure</i> replication tests</li> <li>• Begin <i>mitigation</i> phase submerged testing</li> </ul>
<p>Execute Scaled Testing Plan,</p>	<p>September 2019</p>	<ul style="list-style-type: none"> <li>• Complete <i>mitigation</i> phase submerged testing</li> </ul>
<p>Conclude RCA Execute Scaled Testing Plan,</p>	<p>October 2019</p>	<ul style="list-style-type: none"> <li>• Begin <i>validation</i> (of RCA solution for Isolator) phase and complete scaled testing mitigation phase</li> <li>• Large-team SME reviews are held over 1 week in Florida</li> <li>• RCA close-out report is prepared &amp; tradestudy of go-forward options is completed</li> </ul>
<p>Execute Scaled Testing Plan, Wrap up Test Program</p>	<p>Nov &amp; Dec 2019</p>	<ul style="list-style-type: none"> <li>• Complete <i>validation</i> phase testing</li> <li>• Wind down the offsite testing program, officially ending in February 2020</li> </ul>

**Table 2: 2019 RCA Major Activities**

From the aforementioned “20191014 ESEIEH [Low](#) Power RCA Failure Replication Report”, the image below (Figure 42) shows the severity of the thermal damage seen on the thermoplastic centre isolator component after it had been removed from the borehole. Deposits of petroleum coke on the downhole completion were also noted as the in situ temperature conditions due to the local electrical arcing event was sufficiently high to crack the bitumen.

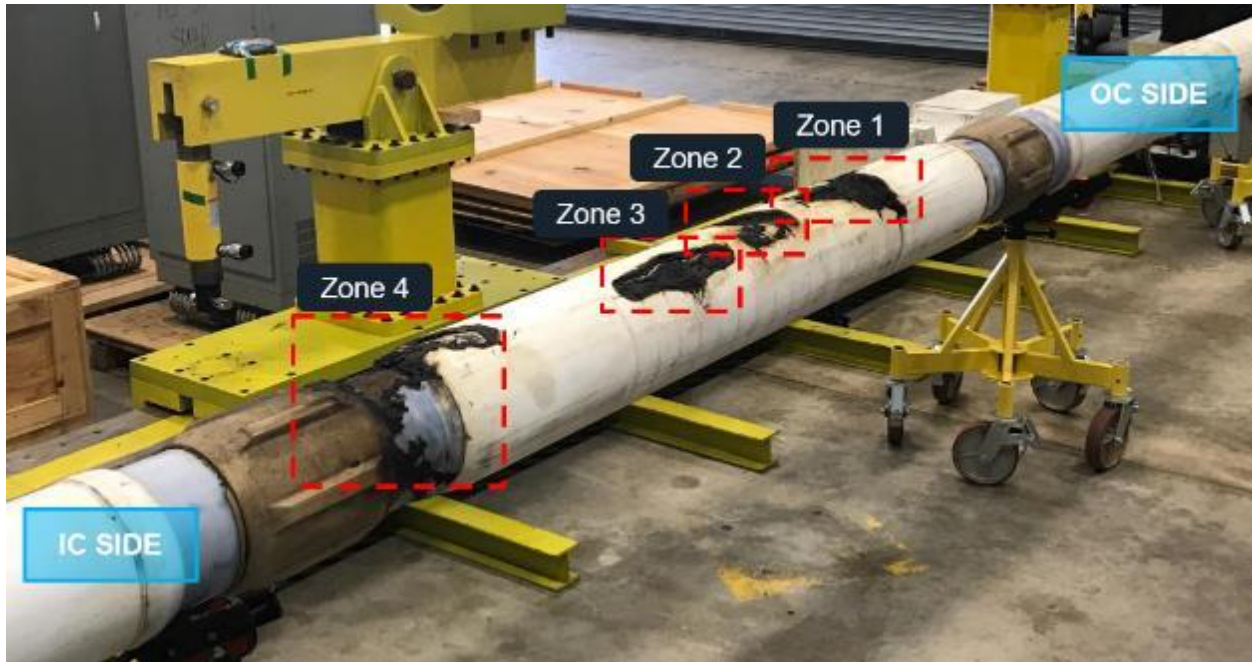


Figure 42: Isolator Damage from 2019 Restart

The *failure replication* portion of the testing program confirmed the probable sequence of events leading to failure as:

1. Field enhancement(s) near the OC side (Heel) corona ring in Zone 1 created high field gradients.
  - Field enhancement likely a combination of a carbon source (bitumen, potassium formate, etc.) with conductive water between PTFE layers.
  - Scaled testing has shown that conductive water between PTFE layers is key to initiate Partial Discharge and when combined with a carbon source results in damage similar to pilot.
  - These conditions were exacerbated by the thermal decay validation of the CEMRS model. By cycling power to the system, salts were accumulated beneath the Teflon sleeve and the conductivity increased with subsequent cycles as the connate water (saline with bitumen) were ingested, evaporated and rewetted. Final conductivities measured near the corona rings on the isolator assemblies were as high as 60 Siemens/Meter.
2. The high field gradients resulted in partial discharge initiation, which led to electrical tracking on PTFE layer 2 that migrated from the bottom to top of OC side corona feature in Zone 1.
3. Partial discharge eroded thru PTFE sleeve on both the top and bottom of OC side (Zone 1) resulting in the exposure of the OC metal electrode to the external environment.
4. The exposed OC initiated a conductive path, and subsequent arc, in the reservoir from the OC side (Zone 1) to the IC side (Zone 4) along the top of the isolator.
  - High temperatures as a result of creating the conductive path overheated the adjacent reservoir.

- Thermal damage to the PTFE indicates temperatures in excess of 450°C
  - This event created external thermal damage on the isolator (Zones 2 and 3).
  - No evidence of conductive path connecting Zones 2 and 3.
  - No evidence of conductive path between PTFE layers or on the phenolic.
5. Conductive path and subsequent arc terminated at the IC side of the antenna (Zone 4).
- Evidence of puncture damage to the PTFE sleeve at this location during manufacturing.

### ***Proposed Restart***

In October 2019, Harris proposed a pilot plan restart that would have re-designed a single stage antenna to be re-installed at the Dover test site. Harris had requested a review of the total go-forward budget to re-start Dover pilot in late 2020 as proposed.

The primary objective for the Dover restart plan was proposed to be a proof of the reliability and ability to impart EM Heating over roughly a 6-9 month period, with the budget and activities to test solvent recovery to be considered secondary to the primary objective of establishing antenna heating reliability.

It was estimated that the existing scheduled activities to redesign and test a new single-stage isolator and execute 6-8 months of heating would entail a budget (100% WI) of \$10-12MM CDN.

The ESEIEH® management committee requested that the technical committees work towards refining this estimate as well as review any new implications with respect to the previously evaluated re-start alternatives.

The request for incremental funding from the ESEIEH® consortium was not successful, and the project restart was placed on indefinite hold, pending future interest and capital availability from Suncor and project partners. As per the MC meeting minutes of Dec 2019 attached, CNOOC and CNRL (which had acquired Devon's interest) both indicated they were withdrawing from the ESEIEH® consortium. The final decision for CNOOC and CNRL to withdraw from the ESEIEH® consortium is captured in the attached "ESEIEH® Mail Ballots 2019-12-6" documentation.

### ***Mitigation Testing***

Throughout Q4 2019, Suncor continued to fund low- and high-voltage testing of various prototypes by Harris at Malabar to further understand design factor sensitivities to field operating conditions with the ultimate goal of selecting a robust final design. Key findings from this work include:

- The mitigation steps to prevent PD initiation and arcing:
  1. Prevent field intensification and carbon sourcing
    - Eliminate connate water intrusion. Connate water is a highly conductive fluid that contains carbon which can initiate PD and propagate arcing. Eliminating the source of these two components eliminates the onset of PD and the propagation of arcing. There are currently several candidate design modifications under consideration to accomplish this. The Small Scale test program final phase is to physical test each of these modifications to select a final design for commercial application.
  2. Prevent field intensity sufficient for PD onset

- Field intensity can be controlled by several factors
  - Coating thickness is a primary factor to control PD onset external to coating; deploy with thickest effective coating achievable which may be accomplished either by mechanical thickness (or inflation) or by introducing an external conditioning fluid.
  - Control peak field intensity via controlled power at startup (until the region is fully desiccated). The field intensity at which PD begins has not yet been validated. The Malabar testing was terminated due to onset of the COVID 19 pandemic before this value was measured. Restarting the technology development should begin with the completion of this measurement.

Scaled testing with thick isolator in oil sands successfully completed the desiccation process without PD validating the primary mitigation design modification.

### ***Post-Partner Funding Period***

The Test Program in Malabar, Florida was ultimately stood down in February 2020 due to lack of funding commitment from Partners and the onset of the COVID 19 pandemic. Verification testing of a scaled prototype which incorporates the test program learnings into a final engineering design is outstanding.

In December 2021, TerraVent reached an Agreement with Harris to purchase the technology assets and intellectual property; the active Project Agreements with Suncor were also transferred from Harris to TerraVent.

In Q1 2022, Suncor and TerraVent jointly made the decision to terminate the ESEIEH® Project and pivot to abandonment and reclamation activity. There is general alignment that given the previous failures and high number of intervention operations, the current wellbore and reservoir section is no longer suitable for further testing. Petroleum Coke, load volumes of injected diesel, and various FOD, such as metal shavings may all be present in the vicinity of the existing antenna well; the option of re-drilling the wellbore to avoid the disturbed and problematic reservoir zone was de-selected as it would place the new well outside the array of other wells and the solvent injection well. Additionally, it was determined by both Companies that a successful field demonstration at Dover would require a follow-up commercial-length trial to sufficiently de-risk the heating effectiveness of the technology.

Suncor has no future plans to continue funding the development of the ESEIEH® technology, in part due to competing interests in development of alternative In Situ recovery processes. However, TerraVent intends to resume the R&D program aimed at prototype design testing and advancing full-scale field piloting options.

The Project Abandonment and Reclamation planning is in-flight and field operations are expected to commence in Q3 2022 – surface facility removal and wellbore abandonment may be completed in 2022, while reclamation will take several years to achieve.

## F. Overall Conclusions

### Scientific Achievements

A general list of significant achievements throughout the project include:

- Validation of electromagnetic energy penetration into native, heterogeneous oil sands
- Both in the Mine Face Test and the 2019 Pilot restart
- First field validation of a simulation tool (CEMRS™) capable of predicting temperature profiles, penetration and heating rates by electromagnetic energy in a hydrocarbon resource
- Both in the Mine Face Test and the Pilot
- Demonstrated change in produce fluids from the use of electromagnetic heating in produced fluids
- Demonstrated use of standard facility design processes and materials in electromagnetically based systems on surface and subsurface systems
- Demonstrated and documented safety procedures and protocols for electromagnetic systems
- Produced significant technical innovations documented in Table 3, Project Related Patents.

Suncor, its Partners in ESEIEH®, and a number of other Academics (e.g. Evaluation of energy and GHG emissions' footprints of bitumen extraction using Enhanced Solvent Extraction Incorporating Electromagnetic Heating technology) have independently completed Life Cycle Analysis of the GHG intensity of the ESEIEH® process in comparison to a typical SAGD. In general, the reduction in emissions (for a constant volume of oil produced) achieved by applying the ESEIEH® Process is generally ~50-70%. Some of the literature\* suggests a reduction as high as 83% may be achieved with the most environmentally sustainable approach.

Suncor's in-house assessment found a number of controllable and uncontrollable factors that will lower the GHG intensity even further, such as:

Reservoir Performance: Less asphaltene precipitation in situ or better than expected heating and solvent performance could lead to higher oil rates and / or lower solvent recycling ratios (i.e. lower heating requirement for surface separation facility)

- Operating Strategy: Lower reservoir operating pressures create lower temperature chambers, and therefore a more thermally efficient heating process (less heat loss from conduction and reservoir leak off)
- Power grid; a higher mix of renewable power would lower the GHG intensity
- Development Strategies: early well abandonment and ramping down power levels in late-life

The sensitivities associated with these uncontrolled variables is shown in Fig 42. Other sustainability studies completed by Suncor found:

- Physical footprint of an ESEIEH development would be similar to SAGD – no significant benefit
- Makeup water usage (from aquifer) is 90% less than SAGD
- Waste water rate is 100% higher than SAGD, requiring more disposal capacity

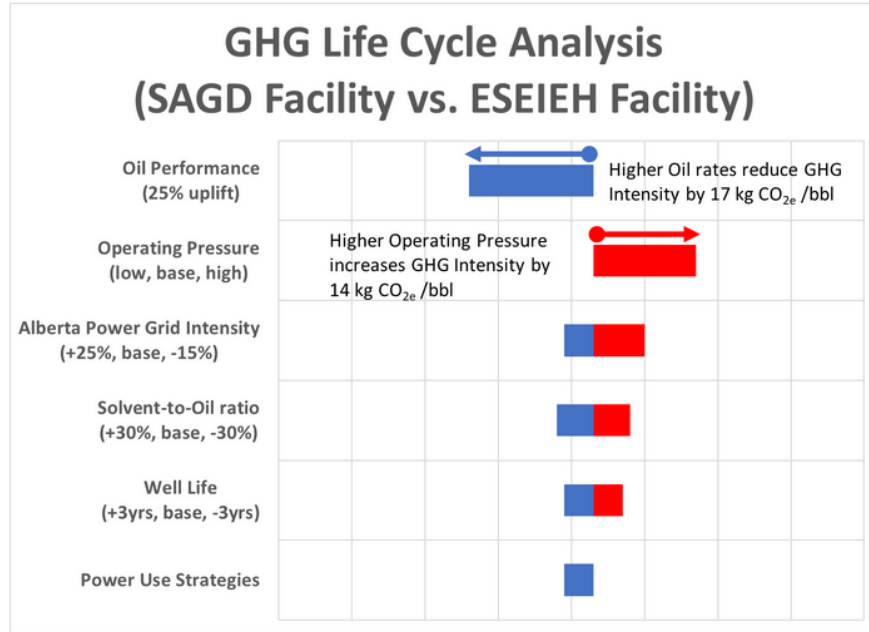


Figure 43: ESEIEH(R) GHG Factor Sensitivities

**Project Related Patents**

Title	Patent No.	Country	Inventors	Hyperlink To Doc
APPARATUS FOR HEATING A HYDROCARBON RESOURCE IN A SUBTERRANEAN FORMATION INCLUDING A FLUID BALUN AND RELATED METHODS	2842300	CA	DITTMER , TIMOTHY W; HIBNER, VERLIN A	<a href="https://www.google.com/patents/US9157305">https://www.google.com/patents/US9157305</a>
APPARATUS FOR HEATING A HYDROCARBON RESOURCE IN A SUBTERRANEAN FORMATION INCLUDING A FLUID BALUN AND RELATED METHODS	9157305	TT	DITTMER , TIMOTHY W; HIBNER, VERLIN A	<a href="https://www.google.com/patents/US9157305">https://www.google.com/patents/US9157305</a>
APPARATUS FOR HEATING A HYDROCARBON RESOURCE IN A SUBTERRANEAN FORMATION INCLUDING A FLUID BALUN AND RELATED METHODS	9157305	US	DITTMER , TIMOTHY W; HIBNER, VERLIN A	<a href="https://www.google.com/patents/US9157305">https://www.google.com/patents/US9157305</a>
APPARATUS FOR HEATING A HYDROCARBON RESOURCE IN A SUBTERRANEAN FORMATION PROVIDING AN ADJUSTABLE LIQUID COOLANT AND RELATED METHODS	9267365	BR	WRIGHT, BRIAN N; TRAUTMAN, MARK A; HIBNER, VERLIN A; DITTMER , TIMOTHY W	<a href="https://www.google.com/patents/US9267365">https://www.google.com/patents/US9267365</a>

APPARATUS FOR HEATING A HYDROCARBON RESOURCE IN A SUBTERRANEAN FORMATION PROVIDING AN ADJUSTABLE LIQUID COOLANT AND RELATED METHODS	9267365	CA	WRIGHT, BRIAN N; TRAUTMAN, MARK A; HIBNER, VERLIN A; DITTMER, TIMOTHY W	<a href="https://www.google.com/patents/US9267365">https://www.google.com/patents/US9267365</a>
APPARATUS FOR HEATING A HYDROCARBON RESOURCE IN A SUBTERRANEAN FORMATION PROVIDING AN ADJUSTABLE LIQUID COOLANT AND RELATED METHODS	9267365	TT	WRIGHT, BRIAN N; TRAUTMAN, MARK A; HIBNER, VERLIN A; DITTMER, TIMOTHY W	<a href="https://www.google.com/patents/US9267365">https://www.google.com/patents/US9267365</a>
APPARATUS FOR HEATING A HYDROCARBON RESOURCE IN A SUBTERRANEAN FORMATION PROVIDING AN ADJUSTABLE LIQUID COOLANT AND RELATED METHODS	9267365	US	WRIGHT, BRIAN N; TRAUTMAN, MARK A; HIBNER, VERLIN A; DITTMER, TIMOTHY W	<a href="https://www.google.com/patents/US9267365">https://www.google.com/patents/US9267365</a>
APPARATUS FOR HEATING A HYDROCARBON RESOURCE IN A SUBTERRANEAN FORMATION PROVIDING AN ADJUSTABLE LIQUID COOLANT AND RELATED METHODS	104005745A	CN	WRIGHT, BRIAN N; TRAUTMAN, MARK A; HIBNER, VERLIN A; DITTMER, TIMOTHY W	<a href="https://www.google.com/patents/CN104005745A">https://www.google.com/patents/CN104005745A</a>
EFFECTIVE SOLVENT EXTRACTION SYSTEM INCORPORATING ELECTROMAGNETIC HEATING	2816297	CA	TRAUTMAN, MARK A; EHRESMAN, DERIK T; EDMUNDS, NEIL; TAYLOR, GEORGE; CIMOLAI, MAURO	<a href="https://patents.google.com/patent/CA2816297A1/en?q=CA2816297">https://patents.google.com/patent/CA2816297A1/en?q=CA2816297</a>
EFFECTIVE SOLVENT EXTRACTION SYSTEM INCORPORATING ELECTROMAGNETIC HEATING	8616273	US	TRAUTMAN, MARK A; EHRESMAN, DERIK T; EDMUNDS, NEIL; TAYLOR, GEORGE; CIMOLAI, MAURO	<a href="https://patents.google.com/patent/US8616273B2/en?q=8616273">https://patents.google.com/patent/US8616273B2/en?q=8616273</a>
EFFECTIVE SOLVENT EXTRACTION SYSTEM INCORPORATING ELECTROMAGNETIC HEATING	2010363970	AU	TRAUTMAN, MARK A; EHRESMAN, DERIK T; EDMUNDS, NEIL; TAYLOR, GEORGE; CIMOLAI, MAURO	<a href="https://www.google.com/patents/WO2012067613A1">https://www.google.com/patents/WO2012067613A1</a>
HYDROCARBON RESOURCE HEATING APPARATUS INCLUDING RF CONTACTS AND ANCHORING DEVICE AND RELATED METHODS	20150129224	CA	WRIGHT, BRIAN N; HEWIT, RAYMOND C; HANN, MURRAY T; WATT (NON-HARRIS), ALAN F; LINKEWICH (NON-HARRIS), ZACHARY L	<a href="https://www.google.com/patents/US20150129224">20150129224https://www.google.com/patents/US20150129224</a>
HYDROCARBON RESOURCE HEATING APPARATUS INCLUDING RF CONTACTS AND ANCHORING DEVICE AND RELATED METHODS	20150129224	US	WRIGHT, BRIAN N; HEWIT, RAYMOND C; HANN, MURRAY T; WATT (NON-HARRIS), ALAN F; LINKEWICH (NON-HARRIS), ZACHARY L	<a href="https://www.google.com/patents/US20150129224">https://www.google.com/patents/US20150129224</a>

HYDROCARBON RESOURCE HEATING SYSTEM INCLUDING COMMON MODE CHOKE ASSEMBLY AND RELATED METHODS	2877929	CA	WRIGHT, BRIAN N; HEWIT, RAYMOND C; HANN, MURRAY T; HIBNER, VERLIN A; TRAUTMAN, MARK A; WHITE (NON-HARRIS), JOHN E	<a href="https://www.google.com/patents/CA2877929A1">https://www.google.com/patents/CA2877929A1</a>
HYDROCARBON RESOURCE HEATING SYSTEM INCLUDING COMMON MODE CHOKE ASSEMBLY AND RELATED METHODS	9441472	US	WRIGHT, BRIAN N; HEWIT, RAYMOND C; HANN, MURRAY T; HIBNER, VERLIN A; TRAUTMAN, MARK A; WHITE (NON-HARRIS), JOHN E	<a href="https://www.google.com/patents/US20150211336">https://www.google.com/patents/US20150211336</a>
HYDROCARBON RESOURCE HEATING SYSTEM INCLUDING COMMON MODE CHOKE ASSEMBLY AND RELATED METHODS	104806216	CN	WRIGHT, BRIAN N; HEWIT, RAYMOND C; HANN, MURRAY T; HIBNER, VERLIN A; TRAUTMAN, MARK A; WHITE (NON-HARRIS), JOHN E	<a href="https://www.google.com/patents/CN104806216A">https://www.google.com/patents/CN104806216A</a>
HYDROCARBON RESOURCE HEATING SYSTEM INCLUDING COMMON MODE CHOKE ASSEMBLY AND RELATED METHODS	2015211336	BR	WRIGHT, BRIAN N; HEWIT, RAYMOND C; HANN, MURRAY T; HIBNER, VERLIN A; TRAUTMAN, MARK A; WHITE (NON-HARRIS), JOHN E	<a href="https://www.google.com/patents/US20150211336">https://www.google.com/patents/US20150211336</a>
HYDROCARBON RESOURCE PROCESSING APPARATUS FOR GENERATING A TURBULENT FLOW OF COOLING LIQUID AND RELATED METHODS	2922158	CA	HANN, MURRAY T; WRIGHT, BRIAN N; WHITE (NON-HARRIS), JOHN E; TRAUTMAN, MARK A	<a href="https://www.google.com/patents/CA2922159A1">https://www.google.com/patents/CA2922159A1</a>
HYDROCARBON RESOURCE PROCESSING APPARATUS FOR GENERATING A TURBULENT FLOW OF COOLING LIQUID AND RELATED METHODS	9474108	US	HANN, MURRAY T; WRIGHT, BRIAN N; WHITE (NON-HARRIS), JOHN E; TRAUTMAN, MARK A	<a href="https://www.google.com/patents/US20150068706">https://www.google.com/patents/US20150068706</a>
METHOD OF UPGRADING AND RECOVERING A HYDROCARBON RESOURCE FOR PIPELINE TRANSPORT AND RELATED SYSTEM	2819654	CA	BLUE, MARK E; TOMAZINIS, CALEB B; SMITH, SCOTT S	<a href="https://www.google.com/patents/CA2819654C">https://www.google.com/patents/CA2819654C</a>
METHOD OF UPGRADING AND RECOVERING A HYDROCARBON RESOURCE FOR PIPELINE TRANSPORT AND RELATED SYSTEM	20140014326	RU	BLUE, MARK E; TOMAZINIS, CALEB B; SMITH, SCOTT S	<a href="https://www.google.com/patents/US20140014326">https://www.google.com/patents/US20140014326</a>

METHOD OF UPGRADING AND RECOVERING A HYDROCARBON RESOURCE FOR PIPELINE TRANSPORT AND RELATED SYSTEM	20140014326	US	BLUE, MARK E; TOMAZINIS, CALEB B; SMITH, SCOTT S	<a href="https://www.google.com/patents/US20140014326">https://www.google.com/patents/US20140014326</a>
RADIO FREQUENCY ANTENNA ASSEMBLY FOR HYDROCARBON RESOURCE RECOVERY INCLUDING ADJUSTABLE SHORTING PLUG AND RELATED METHODS	2843714	CA	WRIGHT, BRIAN N; HANN, MURRAY T; HIBNER, VERLIN A; HEWIT, RAYMOND C	<a href="https://www.google.com/patents/CA2843714A1">https://www.google.com/patents/CA2843714A1</a>
RADIO FREQUENCY ANTENNA ASSEMBLY FOR HYDROCARBON RESOURCE RECOVERY INCLUDING ADJUSTABLE SHORTING PLUG AND RELATED METHODS	9309757	TT	WRIGHT, BRIAN N; HANN, MURRAY T; HIBNER, VERLIN A; HEWIT, RAYMOND C	<a href="https://www.google.com/patents/US9309757">https://www.google.com/patents/US9309757</a>
RADIO FREQUENCY ANTENNA ASSEMBLY FOR HYDROCARBON RESOURCE RECOVERY INCLUDING ADJUSTABLE SHORTING PLUG AND RELATED METHODS	9309757	US	WRIGHT, BRIAN N; HANN, MURRAY T; HIBNER, VERLIN A; HEWIT, RAYMOND C	<a href="https://www.google.com/patents/US9309757">https://www.google.com/patents/US9309757</a>
RADIO FREQUENCY ANTENNA ASSEMBLY FOR HYDROCARBON RESOURCE RECOVERY INCLUDING ADJUSTABLE SHORTING PLUG AND RELATED METHODS	20160194943	US	WRIGHT, BRIAN N; HANN, MURRAY T; HIBNER, VERLIN A; HEWIT, RAYMOND C	<a href="https://www.google.com/patents/US20160194943">https://www.google.com/patents/US20160194943</a>
RF ANTENNA ASSEMBLY INCLUDING DUAL-WALL CONDUCTOR AND RELATED METHODS	9016367	US	HANN, MURRAY T; WRIGHT, BRIAN N; NUGENT, KEITH	<a href="https://www.google.com/patents/US9016367">https://www.google.com/patents/US9016367</a>
RF ANTENNA ASSEMBLY WITH DIELECTRIC ISOLATOR AND RELATED METHODS (consists of 6 breakouts: Breakout #1 METHOD FOR ASSEMBLING A SUBSURFACE CENTER FED DIPOLE POWER NODE)	2847366	CA	WRIGHT, BRIAN N; HANN, MURRAY T; HIBNER, VERLIN A; HEWIT, RAYMOND C	<a href="https://www.google.com/patents/CA2847366A1">https://www.google.com/patents/CA2847366A1</a>
RF ANTENNA ASSEMBLY WITH DIELECTRIC ISOLATOR AND RELATED METHODS (consists of 6 breakouts: Breakout #1 METHOD FOR ASSEMBLING A SUBSURFACE CENTER FED DIPOLE POWER NODE)	9322256	TT	WRIGHT, BRIAN N; HANN, MURRAY T; HIBNER, VERLIN A; HEWIT, RAYMOND C	<a href="https://www.google.com/patents/US9322256">https://www.google.com/patents/US9322256</a>
RF ANTENNA ASSEMBLY WITH DIELECTRIC ISOLATOR AND RELATED METHODS (consists of 6 breakouts: Breakout #1 METHOD FOR ASSEMBLING A SUBSURFACE CENTER FED DIPOLE POWER NODE)	9322256	US	WRIGHT, BRIAN N; HANN, MURRAY T; HIBNER, VERLIN A; HEWIT, RAYMOND C	<a href="https://www.google.com/patents/US9322256">https://www.google.com/patents/US9322256</a>
RF ANTENNA ASSEMBLY WITH FEED STRUCTURE HAVING DIELECTRIC TUBE AND RELATED METHODS	2896258	CA	AYERS, SCHUYLER R; HANN, MURRAY T; WRIGHT, BRIAN N; HIBNER, VERLIN A; DITTMER, TIMOTHY W	<a href="https://www.google.com/patents/CA2896258A1">https://www.google.com/patents/CA2896258A1</a>

RF ANTENNA ASSEMBLY WITH FEED STRUCTURE HAVING DIELECTRIC TUBE AND RELATED METHODS	9376897	US	AYERS, SCHUYLER R; HANN, MURRAY T; WRIGHT, BRIAN N; HIBNER, VERLIN A; DITTMER, TIMOTHY W	<a href="https://www.google.com/patents/US9376897">https://www.google.com/patents/US9376897</a>
RF ANTENNA ASSEMBLY WITH FEED STRUCTURE HAVING DIELECTRIC TUBE AND RELATED METHODS	2014244124	AU	AYERS, SCHUYLER R; HANN, MURRAY T; WRIGHT, BRIAN N; HIBNER, VERLIN A; DITTMER, TIMOTHY W	<a href="https://www.google.com/patents/WO2014160137A1">https://www.google.com/patents/WO2014160137A1</a>
RF ANTENNA ASSEMBLY WITH SERIES DIPOLE ANTENNAS AND COUPLING STRUCTURE AND RELATED METHODS (spin from GCSD-2557 consists of 6 breakouts: Breakout #2 COLLINEAR COAXIAL ANTENNA SYSTEM FOR SUBTERRANEAN HYDROCARBONS HEATING AND RECOVERY)	2847365	CA	WRIGHT, BRIAN N; HANN, MURRAY T; HEWIT, RAYMOND C; JACKSON, JR., RONALD E	<a href="https://www.google.com/patents/CA2847365A1">https://www.google.com/patents/CA2847365A1</a>
RF ANTENNA ASSEMBLY WITH SERIES DIPOLE ANTENNAS AND COUPLING STRUCTURE AND RELATED METHODS (spin from GCSD-2557 consists of 6 breakouts: Breakout #2 COLLINEAR COAXIAL ANTENNA SYSTEM FOR SUBTERRANEAN HYDROCARBONS HEATING AND RECOVERY)	9181787	US	WRIGHT, BRIAN N; HANN, MURRAY T; HEWIT, RAYMOND C; JACKSON, JR., RONALD E	<a href="https://www.google.com/patents/US9181787">https://www.google.com/patents/US9181787</a>
RF ANTENNA ASSEMBLY WITH SPACER AND SHEATH AND RELATED METHODS (spin from GCSD-2557 consists of 6 breakouts: Breakout #4 METHOD FOR AXIAL & RADIAL SUPPORTING A TRANSMISSION LINE WITHIN A SUBSURFACE BALUN OR TRANSDUCER ELEMENT)	2922793	CA	WRIGHT, BRIAN N; HANN, MURRAY T; HEWIT, RAYMOND C	<a href="https://www.google.com/patents/WO2015047540A1">https://www.google.com/patents/WO2015047540A1</a>
RF ANTENNA ASSEMBLY WITH SPACER AND SHEATH AND RELATED METHODS (spin from GCSD-2557 consists of 6 breakouts: Breakout #4 METHOD FOR AXIAL & RADIAL SUPPORTING A TRANSMISSION LINE WITHIN A SUBSURFACE BALUN OR TRANSDUCER ELEMENT)	9376899	US	WRIGHT, BRIAN N; HANN, MURRAY T; HEWIT, RAYMOND C	<a href="https://www.google.com/patents/US9376899">https://www.google.com/patents/US9376899</a>
RF COAXIAL TRANSMISSION LINE FOR A WELLBORE INCLUDING DUAL-WALL OUTER CONDUCTOR AND RELATED METHODS	9458708	US	WRIGHT, BRIAN N; HEWIT, RAYMOND C; NUGENT, KEITH	<a href="https://www.google.com/patents/US20140041890">https://www.google.com/patents/US20140041890</a>
RIGID RF COXIAL TRANSMISSION LINE WITH CONNECTOR HAVING ELECTRICALLY CONDUCTIVE LINER AND RELATED METHODS (spin from GCSD-2557 consists of 6 breakouts: Breakout #5 ALUMINUM TUBULARS FOR STRUCTURAL COAX FOR SUBTERRANEAN HYDROCARBONS HEATING AND RECOVERY)	2922791	CA	WRIGHT, BRIAN N; HANN, MURRAY T; HEWIT, RAYMOND C; WHITNEY, RYAN M	<a href="https://www.google.com/patents/CA2922791A1">https://www.google.com/patents/CA2922791A1</a>

RIGID RF COXIAL TRANSMISSION LINE WITH CONNECTOR HAVING ELECTRICALLY CONDUCTIVE LINER AND RELATED METHODS (spin from GCSD-2557 consists of 6 breakouts: Breakout #5 ALUMINUM TUBULARS FOR STRUCTURAL COAX FOR SUBTERRANEAN HYDROCARBONS HEATING AND RECOVERY)	9377553	US	WRIGHT, BRIAN N; HANN, MURRAY T; HEWIT, RAYMOND C; WHITNEY, RYAN M	<a href="https://www.google.com/patents/US9377553">https://www.google.com/patents/US9377553</a>
SUBTERRANEAN ANTENNA INCLUDING ANTENNA ELEMENT AND COAXIAL LINE THEREIN AND RELATED METHODS	2875100	CA	WRIGHT, BRIAN N; DICKEY (NON-HARRIS), DANIEL L; HEWIT, RAYMOND C	<a href="https://www.google.com/patents/CA2875100A1">https://www.google.com/patents/CA2875100A1</a>
SUBTERRANEAN ANTENNA INCLUDING ANTENNA ELEMENT AND COAXIAL LINE THEREIN AND RELATED METHODS	02013192124	TT	WRIGHT, BRIAN N; DICKEY (NON-HARRIS), DANIEL L; HEWIT, RAYMOND C	<a href="https://www.google.com/patents/WO2013192124A3">https://www.google.com/patents/WO2013192124A3</a>
SUBTERRANEAN ANTENNA INCLUDING ANTENNA ELEMENT AND COAXIAL LINE THEREIN AND RELATED METHODS	20130334205	US	WRIGHT, BRIAN N; DICKEY (NON-HARRIS), DANIEL L; HEWIT, RAYMOND C	<a href="https://www.google.com/patents/US20130334205">https://www.google.com/patents/US20130334205</a>

**Table 3: Project Related Patents**

- Project Related Publications

Year	Event/ Publication	Abbr.	Article Reference Number	Title	Author	Link
2015	World Heavy Oil Congress	WHOC	WHOC15-317	Techniques for installing Effective Solvent Extraction Incorporating Electromagnetic Heating ("ESEIEH®") Completions	Shirish R. Despande, Brian N. Wright, Alan Watt	
2016	SPE Canada Heavy Oil Technical Conference	CHOTC	SPE-180729- MS	Reducing Supply Cost with ESEIEH® Pronounced Easy	Spence Wise, Chris Patterson	
2016	World Heavy Oil Congress	WHOC	WHOC16-604	Analysis of Down-Hole Piping Structural Loading	Rick Harless	<a href="https://www.spe.org/en/jpt/jpt-article-detail/?art=1181">https://www.spe.org/en/jpt/jpt-article-detail/?art=1181</a>
2015	Journal of Petroleum Technology (SEPT)	JPT	N/A	Testing Heavy Oil Production Without Steam Heating	Stephen Rassenfoss	<a href="https://www.onepetro.org/journal-paper/SPE-0912-0034-JPT?sort=&amp;start=0&amp;q=eseieh&amp;from_year=2010&amp;peer_reviewed=&amp;published_between=on&amp;fromSearchResults=true&amp;to_year=&amp;rows=10#">https://www.onepetro.org/journal-paper/SPE-0912-0034-JPT?sort=&amp;start=0&amp;q=eseieh&amp;from_year=2010&amp;peer_reviewed=&amp;published_between=on&amp;fromSearchResults=true&amp;to_year=&amp;rows=10#</a>
2012	Journal of Petroleum Technology (SEPT)	JPT	N/A	Oil Sands Get Wired - Seeking More Oil, Fewer Emissions	Stephen Rassenfoss	

**Table 4: Project Related Publications**

### Next Steps

TerraVent is not currently working on a specific timeline but more on a sequence of milestones. The company has only had control of assets since late December, 2021 (about 5 months) and is pressing forward under two parallel efforts until one dominates. The two paths are to grow TerraVent either at the pace allowed by our own project plan or at an accelerated pace with external investment. The major Milestones may be viewed in Figure 43. Progress in advancing the technology will be posted on the TerraVent website.

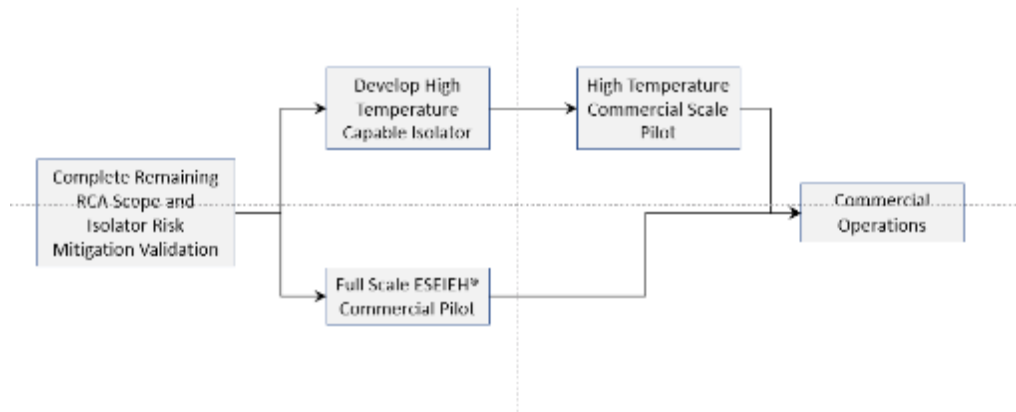


**Figure 44: TerraVent Environmental Next Steps**

### ***Communications Plan***

During the ESEIEH® project, a number of communications efforts were undertaken by the project team both within and outside the project. Table 4 lists the publications related to the project but there were also a number of radio and news interviews outside the required public progress report including the Calgary Herald (9.29.15), Wall Street Journal (7.24.12), Scientific American, Globe and Mail (6.13.12), Rigzone (7.13.12), Oil & Gas Journal (6.2012), and others. Additionally, the project was also included in testimony by Mr. Eddie Isaacs, Executive Director of Alberta Innovates, to the US Committee on Energy and Commerce, US House of Representatives on 20 March, 2012 as an example of North American cooperation in energy advancement.:

“New technologies are emerging that are poised to significantly reduce energy intensity, reduce water use and greenhouse gases. These include steam-solvent hybrid processes that are being applied at least by one company commercially today. Use of solvents without steam, you will be hearing about that from Dr. Nenniger and N - Solv is a good example of this type of technology. Electric heating and electromagnetic heating technology is coming into use. Electromagnetic uses radio frequency to heat the oil in the oil sands. These are early days for the electromagnetic heating technology which really does bring the knowhow of the Harris Corporation in radio communication technology with the reservoir expertise of oil sands producers and is a great example of cross -border collaborative effort on a new, innovative, next- generation technology.”

Looking forward, TerraVent intends to continue in a similar vein leveraging news, radio, broadcast and other media. Additionally, TerraVent is currently using digital platforms to inform the industry and general public about the company, its technologies and endeavours. As is typical in today’s business world, the primary site is a business webpage (Located at <https://www.terra-vent.com/>). The webpage is intended to be the primary form of communication and marketing for TerraVent. To channel users of other platforms towards the website, pages have been established on LinkedIn (<https://www.linkedin.com/company/72180918/admin/>) and Twitter (<https://twitter.com/TerraVentEnvr>). The website currently includes biographical information about the TerraVent team, general information about the company, the technology, and some early marketing materials along with a method to contact the company. As progress is made, the website will be maintained and awareness circulated via LinkedIn and Twitter.